AD-A144 215 TAPE CASTING OF HONEYWELL PZT TYPE III POWDER(U) 1/1
PENNSYLVANIA STATE UNIV UNIVERSITY PARK MATERIALS
RESEARCH LAB J V BIGGERS ET AL. FEB 84
UNCLASSIFIED N00014-82-C-0231 F/G 11/2 NL

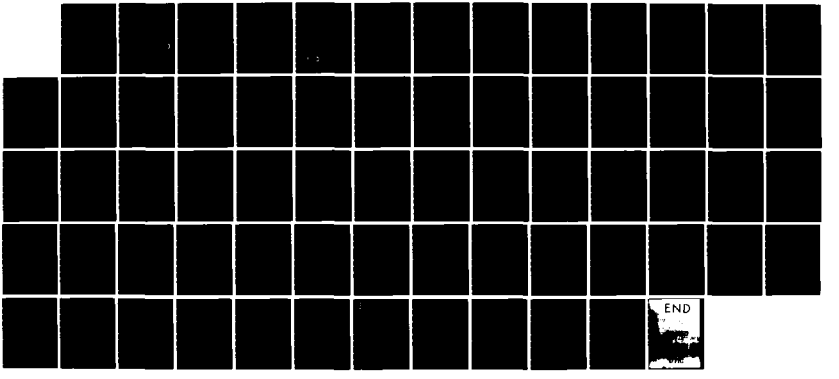

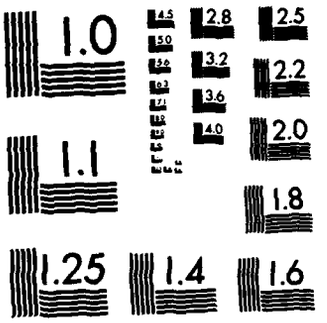

(1)

# IV. Tape Casting of Honeywell PZT Type III Powder

Gordon O. Dayton

Beth A. Jones

James V. Biggers

Final Report on Navy Contract
No. N00014-82-C-0231



THE MATERIALS RESEARCH LABORATORY

THE PENNSYLVANIA STATE UNIVERSITY

UNIVERSITY PARK, PENNSYLVANIA

SECURITY CLASSIFICATION OF THIS PAGE *(When Data Entered)*

## REPORT DOCUMENTATION PAGE

READ INSTRUCTIONS BEFORE COMPLETING FORM

| | |
|---|---|
| 1. REPORT NUMBER | 2. GOVT ACCESSION NO. AD-A144 215 |
| 3. RECIPIENT'S CATALOG NUMBER | |
| 4. TITLE *(and Subtitle)* IV. Tape Casting of Honeywell PZT Type III Powder | 5. TYPE OF REPORT & PERIOD COVERED Final Report February 1982 - February 1984 |
| | 6. PERFORMING ORG. REPORT NUMBER |
| 7. AUTHOR(s) James V. Biggers, Gordon O. Dayton, Beth A. Jones | 8. CONTRACT OR GRANT NUMBER(s) N00014-82-C-0231 |
| 9. PERFORMING ORGANIZATION NAME AND ADDRESS Materials Research Laboratory, The Pennsylvania State University, University Park, PA 16802 | 10. PROGRAM ELEMENT, PROJECT, TASK AREA & WORK UNIT NUMBERS |
| 11. CONTROLLING OFFICE NAME AND ADDRESS Office of Naval Research, Room 619 Ballston Tower, 800 N. Quincy St., Arlington, VA 22217 | 12. REPORT DATE February 1984 |
| | 13. NUMBER OF PAGES |
| 14. MONITORING AGENCY NAME & ADDRESS*(if different from Controlling Office)* | 15. SECURITY CLASS. *(of this report)* Unclassified |
| | 15a. DECLASSIFICATION/DOWNGRADING SCHEDULE |

16. DISTRIBUTION STATEMENT *(of this Report)*

Reproduction in whole or in part is permitted for any purpose of the United States Government

**DISTRIBUTION STATEMENT A**
**Approved for public release;**
**Distribution Unlimited**

17. DISTRIBUTION STATEMENT *(of the abstract entered in Block 20, if different from Report)*

18. SUPPLEMENTARY NOTES

19. KEY WORDS *(Continue on reverse side if necessary and identify by block number)*

20. ABSTRACT *(Continue on reverse side if necessary and identify by block number)*

This is the fourth and final report in the series dealing with transfer of tape casting technology from The Pennsylvania State University, Materials Research Laboratory to Honeywell Ceramic Center. Earlier reports dealt with basic processing techniques for the preparation of multilayer stacks, equipment design, and a survey of the literature on tape casting. Since the project goals were redefined by the Navy Coordinator, April 11, 1983, this report deals only with characterization of H.C.C. PZT powder, and the process variables

DD FORM 1 JAN 73 1473 EDITION OF 1 NOV 65 IS OBSOLETE

SECURITY CLASSIFICATION OF THIS PAGE *(When Data Entered)*

associated with tape casting of this powder. It was determined that the agglomeration nature of the powder is important to this process and for this reason both reprocessed (at MRL) and as-received powder was used in this study. Thickness, density and shrinkage data are monitored from the casting stage to the green tape, laminate and final multilayer stack. A firing study was conducted on pellet samples of HCC PZT type III powder. The burnout characteristics of the Cladan binder system are characterized using thermo-analytical techniques. Over 100 fett of PZT was prepared for use at Honeywell. Work on alternative binders, fast firing, and low cost electrodes was deleted from the proposed work plan. Some of this work will be continued at MRL under other projects.

TABLE OF CONTENTS

## LIST OF TABLES

### Honeywell PZT Powder Characteristics

## LIST OF FIGURES

## 1.0 Introduction

Honeywell PZT type III powder (batch 4516B) has been used in preparing a data base of tape casting parameters and for preparation of PZT tape for use at Honeywell Ceramics Center. All casting slurries have been prepared using various weight percentages of Cladan CB73115 binder to determine tape, laminate and fired multilayer stack properties as a function of binder content. This binder has been used exclusively at MRL as a good all-purpose system that works well for a variety of powders. Since this work began, Cladan has developed a new binder system (CB73088) for use with channel #5502 PZT. This binder may be better suited for PZT's in general.

As data were generated, it was noted that the slurry viscosity, tape density and fired density of samples was not consistent with previous data on PZT powders tape cast at MRL. It was therefore decided to dry ball mill and sieve the Honeywell powder through 325 mesh. The reprocessed powder was found to give measurably better results in terms of the physical properties of the tape and the fired ceramic.

The results suggest that the agglomerate nature of the powder is important in determining how well particles pack in the cast tape which in turn effects the density of the fired multilayer stack.

To date work has dealt solely with that portion of the processes pertaining to tape casting and fabrication of the multilayer stack. No devices have been prepared with internal electrodes and no electrical properties have been measured.

## 2.0 Rheology of Slurries Prepared from As-Received Powder

Slurries were prepared using as-received PZT powder batch 4516B and Cladan CB73115 one part binder/solvent system. A variety of solid loadings

were used from zero to 75 wt% powder. After batching, the slurry was milled with $ZrO_2$ media in a polyethylene jar for 18 to 24 hours.

Upon completion of the milling step, the slurry was de-aired by placing it on a vibration table at moderate amplitude for 20 to 30 minutes. Viscosity was determined and the slurry was tape-cast as described in Section 3.0.

## 2.1 Slurry Viscosity

Slurry viscosity was determined at room temperature using a Brookfield rheolog model RVT-RL with small sample adapter SC-4 and spindle No. 21/13R. The viscometer was allowed to stabilize for one minute at each measuring rpm. Slurry viscosity as a function of binder content for both increasing and decreasing shear rate (rpm) is given in Table 1. In addition to the first group of slurries at various solids loading and the third group for replication purposes, pure binder was measured in the a) unmixed, b) handshaken, and c) mechanically stirred (1 hr.) condition. The striking change for binder decanted from either an unmixed or poorly mixed bottle points out the importance of careful mixing. Data suggests that a low density, high viscosity component of the system is poured first from an unmixed container. The rheologic behavior of these slurries is non-Newtonian, that is, the viscosity is shear rate dependent. All of the slurries so far measured show pseudoplastic behavior. Their viscosity decreases with increasing shear rate with little or no hysteresis or evidence of a yield stress. An example of the viscosity versus shear rate dependence is shown in Figure 1 for slurry H-13, 70 weight percent PZT.

## 2.2 Shear Thinning Index

The degree of departure from Newtonian behavior increases with increasing solids content of the slurry. The pure binder tested shows very little change in viscosity with shear rate when it is properly mixed. One method of

Table 1. Brookfield* viscosity of slurries prepared from as-received powder at specific shear rates (centepois).

| Slurry No. | Wt% Powder | Spindle rpm (Upper Value) and Shear Rate (Lower Value) | | | | | | | | | | | | | | |
|---|---|---|---|---|---|---|---|---|---|---|---|---|---|---|---|---|
| | | 0.5 | 1.0 | 2.5 | 5.0 | 10 | 20 | 50 | 100 | 50 | 20 | 10 | 5.0 | 2.5 | 1.0 | 0.5 |
| | | .465 | .930 | 2.33 | 4.65 | 9.30 | 18.6 | 46.5 | 93.0 | 46.5 | 18.6 | 9.30 | 4.65 | 2.33 | .950 | .465 |
| H14 | 77.2 | -- | -- | 16.2K | O.S. | | | | | | | | O.S. | 15.6K | 29.5K | 51.0K |
| H10 | 75.0 | 42.0K | 25.5K | 14.8K | O.S. | | | | | | | | O.S. | 14.8K | 25.5K | -- |
| H13 | 70.0 | 12.5K | 7.50K | 4.38K | 3.07K | 2.34K | 1.89K | O.S. | | O.S. | 1.88K | 2.30K | 3.00K | 4.20K | 7.40K | -- |
| H11 | 65.0 | 7.00K | 4.70K | 2.90K | 2.23K | 1.86K | 1.63K | O.S. | | O.S. | 1.63K | 1.85K | 2.21K | 2.81K | 4.30K | -- |
| H12 | 60.0 | 6.00K | 4.00K | 2.38K | 1.79K | 1.48K | 1.27K | O.S. | | O.S. | 1.26K | 1.45K | 1.72K | 2.20K | 3.25K | -- |
| H7 | 55.0 | 3.00K | 2.00K | 1.62K | 1.35K | 1.08K | 975 | 880 | O.S. | 880 | 970 | 1.08K | 1.25K | 1.45K | 2.00K | -- |
| H8 | 50.0 | 2.80K | 2.20K | 1.50K | 1.16K | 1.05K | 915 | 820 | O.S. | 810 | 890 | 975 | 1.10K | 1.03K | 1.70K | -- |
| H9 | 40.0 | -- | 1.00K | 700 | 690 | 660 | 630 | 595 | O.S. | 620 | 640 | 680 | 750 | 800 | 1.00K | -- |
| B1 | 0 | | -- | 3.08K | 2.88K | 2.71K | O.S. | | | (Binder: as-received, unmixed) | | | | | | |
| B2 | 0 | | | -- | 2.20K | 2.15K | 2.08K | O.S. | | (Binder: hand shaken jug, 5 min.) | | | | | | |
| B3 | 0 | | | | -- | 370 | 360 | 343 | 333 | O.S. | (Binder: stirred 1 hr) | | | | | |
| H15 | 70.0 | | -- | 5.45K | 4.00K | 2.73K | 2.34K | O.S. | | O.S. | 3.00K | 2.30K | 3.78K | 5.25K | -- | |
| H17 | 65.0 | | -- | 4.00K | 2.75K | 2.00K | 1.65K | O.S. | | O.S. | 1.63K | 1.98K | 2.40K | 3.20K | -- | |
| H16 | 60.0 | | | -- | 1.55K | 1.30K | 1.14K | 950 | O.S. | 970 | 1.13K | 1.28K | 1.50K | -- | | |
| Full Scale | | 100K | 50K | 20K | 10K | 5K | 2.5K | 1.0K | 500 | 1.0K | 2.5K | 5K | 10K | 20K | 50K | 100K |

*Brookfiled Rheolog Model RVT-RL; Small sample adapter SC-4; Spindle No. 21/13R; Temp. 23±1°C
O.S.: Offscale; -- reading not recorded due to low level or excessive oscillation.

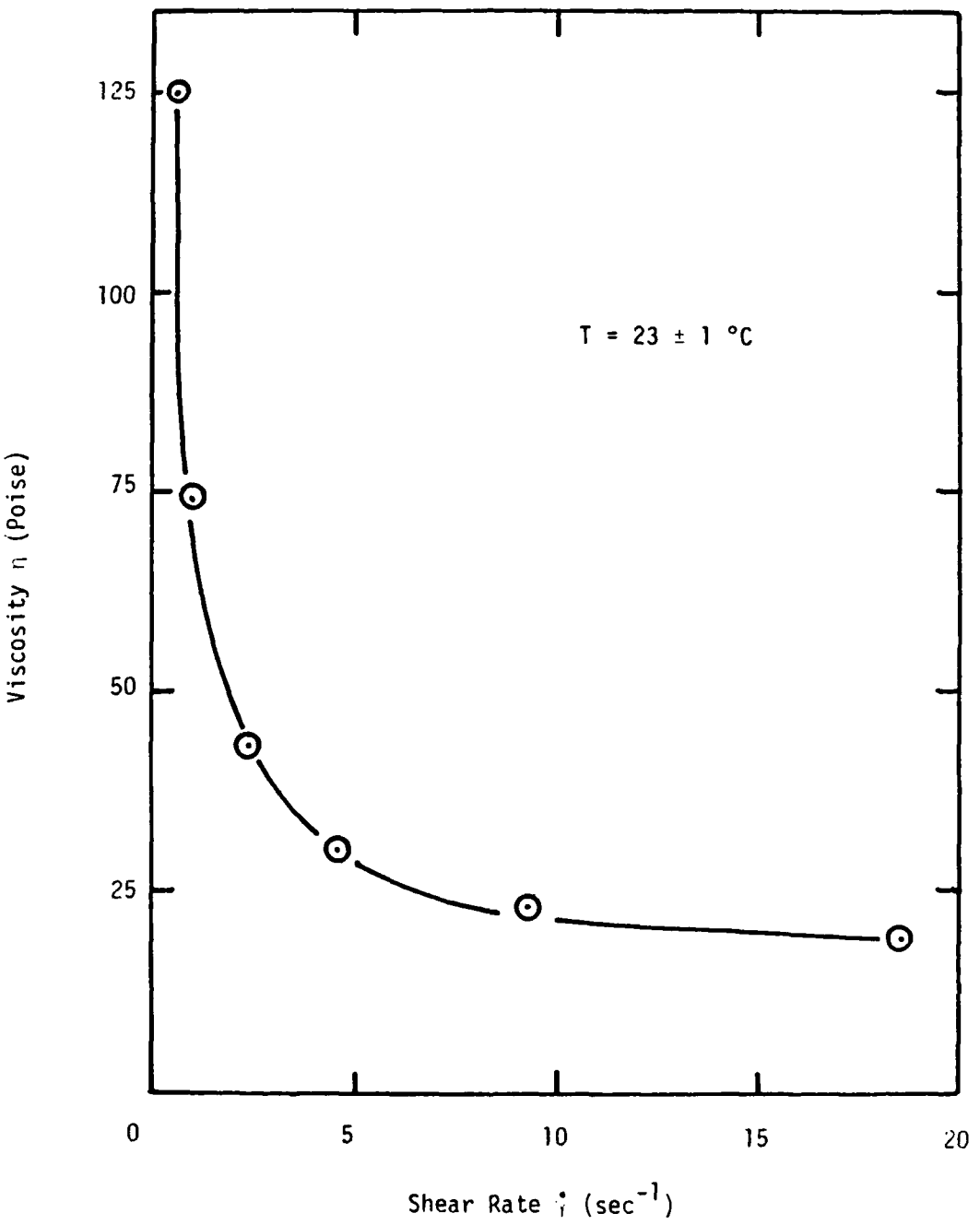
125
100
75
50
25
0
5
10
15
20
T = 23 ± 1 °C
Viscosity η (Poise)
Shear Rate $\dot{\gamma}$ (sec$^{-1}$)

Figure 1.

characterizing the behavior of these slurries is through the determination of the shear thinning index (3) (STI). For a given slurry, a plot of the log of the shear rate versus the log of the shear stress is linear, as shown in Figure 2, and the slope of this plot is the STI. The STI may be defined by

$$STI = \frac{d\ln\dot{\gamma}}{d\ln\tau} \tag{1}$$

where $\dot{\gamma}$ is the shear rate and $\tau$ the shear stress. The behavior of the slurry may be fully described by fitting data to the equation

$$\ln\dot{\gamma} = (STI)\ln\tau + k_o \tag{2}$$

where STI is the slope and k the intercept. Use of this equation allows calculation of viscosity $\eta$ of a given slip composition at any shear rate using the auxilliary equations:

$$\eta = \tau/\dot{\gamma} \tag{3}$$

$$\dot{\gamma} = k' \times rpm \ (sec^{-1}) \tag{4}$$

$$\tau = k'' \times \text{dial reading} \ (dynes/cm^2) \tag{5}$$

for $\eta$ in poise and dial reading in percent of full scale spring deflection. For the viscometer geometry used in our test (Brookfield small sample adapter SC-4, spindle 21 and chamber 13R), $k' = 0.930$ and $k'' = 4.65$[4]. Values of STI and $k_o$ from equation (2) determined from linear regression fitting of data from Table 1 (mean of increasing and decreasing shear rate viscosities used) appear in Table 2.

## 2.3 Dependence of Slip Viscosity on Solids Loading

The dependence of slip viscosity on solids loading at constant shear rate is shown in Figure 3. Sikdar and Ore suggest that the dependence of viscosity

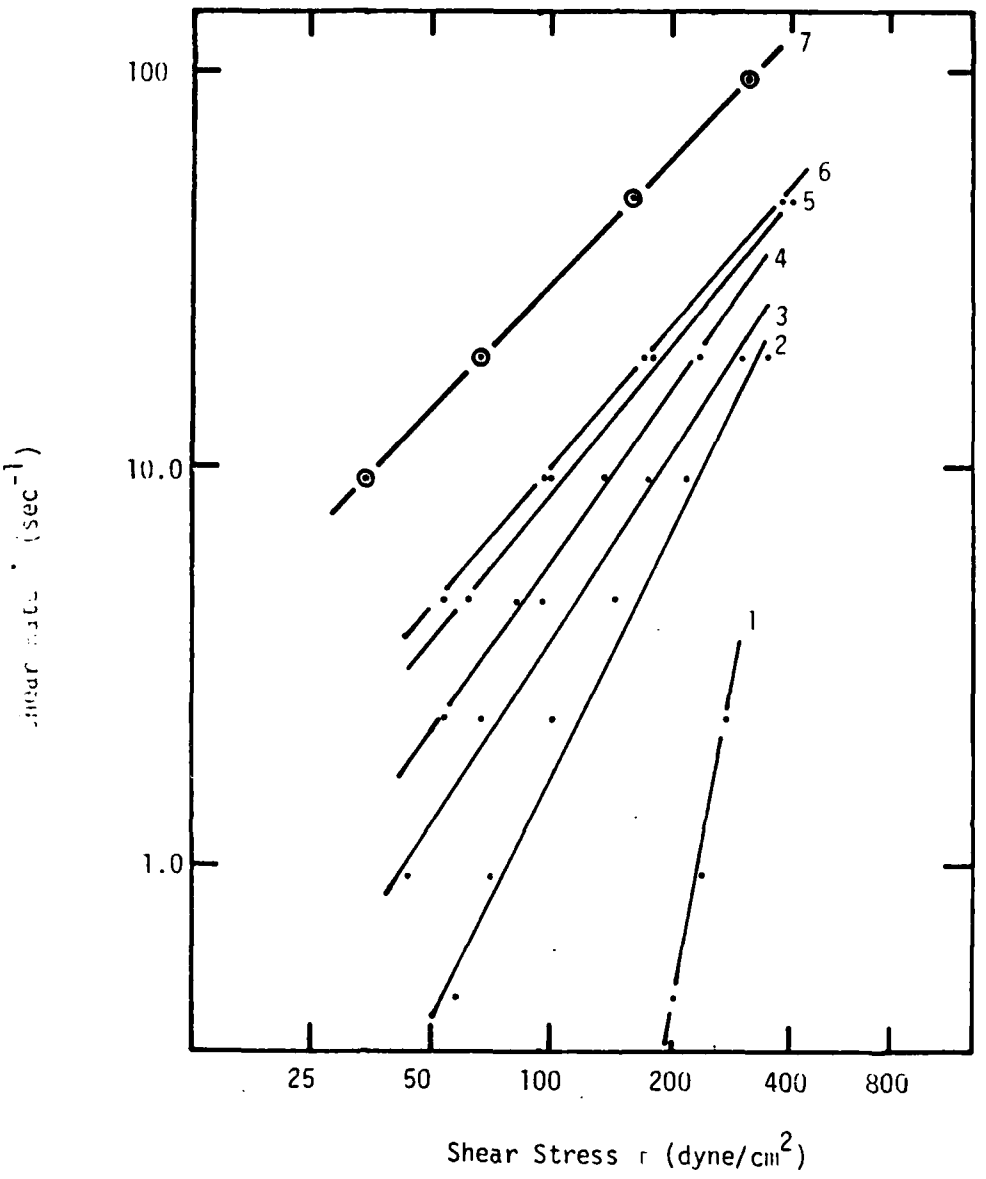
100
10.0
1.0
25
50
100
200
400
800
1
2
3
4
5
6
7
Shear Stress τ (dyne/cm²)

Figure 2.

Table 2. Values of STI and $k_o$ for Honeywell PZT Lot 4561B in Cladan binder CB73115.

| Slip | wt% PZT Powder | Vol% PZT Powder | STI | $k_o$ | $r^{2*}$ |
|---|---|---|---|---|---|
| H-10 | 75 | 27.3 | 2.808 | -15.54 | 0.995 |
| H-13 | 70 | 22.6 | 2.005 | -8.613 | 0.975 |
| H-11 | 65 | 18.8 | 1.622 | -6.164 | 0.982 |
| H-12 | 60 | 15.79 | 1.674 | -6.03 | 0.977 |
| H-7 | 55 | 13.25 | 1.346 | -4.08 | 0.992 |
| H-8 | 50 | 11.11 | 1.333 | -3.907 | 0.988 |
| H-9 | 40 | 7.69 | 1.115 | -2.431 | 0.996 |
| B-3 | 0 | 0 | 1.053 | -1.505 | 1.000 |

*Describes deviation of data about best fit line, 1,000 is perfect fit.

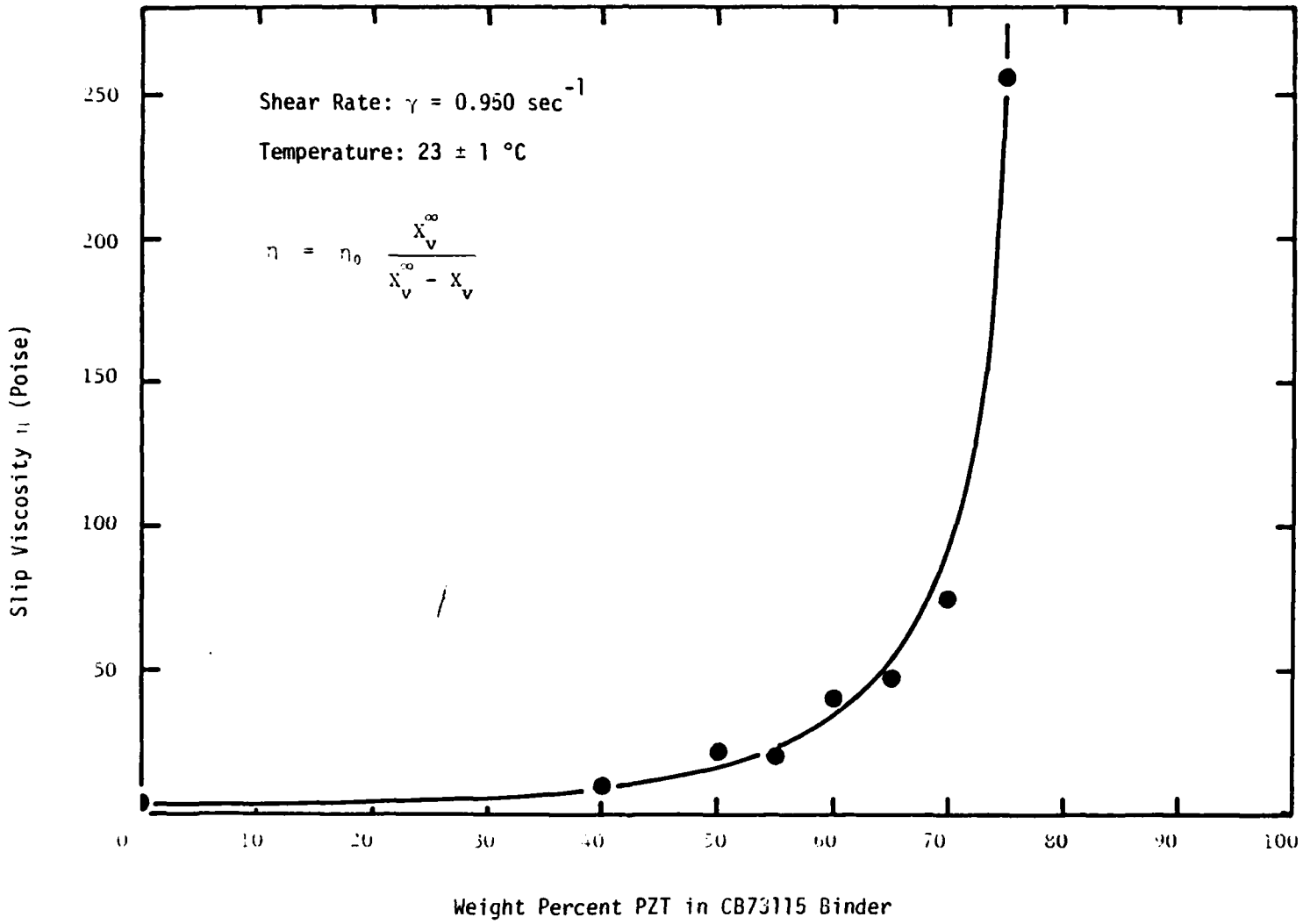
Shear Rate: $\dot{\gamma}$ = 0.950 $sec^{-1}$
Temperature: 23 ± 1 °C
$\eta = \eta_0 \frac{X_v^\infty}{X_v^\infty - X_v}$
Slip Viscosity η (Poise)
250
200
150
100
50
0
10
20
30
40
50
60
70
80
90
100
Weight Percent PZT in CB73115 Binder

Figure 3.

on powder content of a slurry may be described by:

$$\eta = \eta_0 \frac{x_v^\infty}{x_v^\infty - x_v} \tag{6}$$

where $\eta$ is the apparent viscosity, $\eta_0$ the basic viscosity of the suspending medium (binder), $x_v$ the volume fraction solids, and $x_v^\infty$ the volume fraction solids at which viscosity becomes infinite. By rewriting equation (6) as

$$x_v = x_v^\infty \left(\frac{\eta-\eta_0}{\eta}\right) \tag{7}$$

we may evaluate $x_v^\infty$ by a plot of $x_v$ versus $(\eta-\eta_0/\eta)$. This is shown in Figure 4 for data points recalculated using information from Table 3. It can be seen that $x_v^\infty$ is not constant over the entire range of powder loadings, contrary to the findings of Sikdar and Ore. The data does seem linear for powder contents greater than 10 volume percent (~50 weight percent) suggesting that the viscosity relation may be described by the equation:

$$x_v = x_v^\infty \left(\frac{\eta-\eta_0}{\eta}\right) + k_3 \tag{8}$$

over the range of interest. Values of $x_v^\infty$ for these higher solids loading appear in Table 3.

The reason for the deviation in the higher powder content slurries is unclear at present, but may be related to particle size and shape effects of the powder, and increasing particle-liquid interaction at higher solids loadings. Alternatively, it may be related to the measurement geometry which is that of closely spaced coaxial cylinders rather than the more common cylinder-in-an-infinite-liquid geometry. It would seem that the geometry used

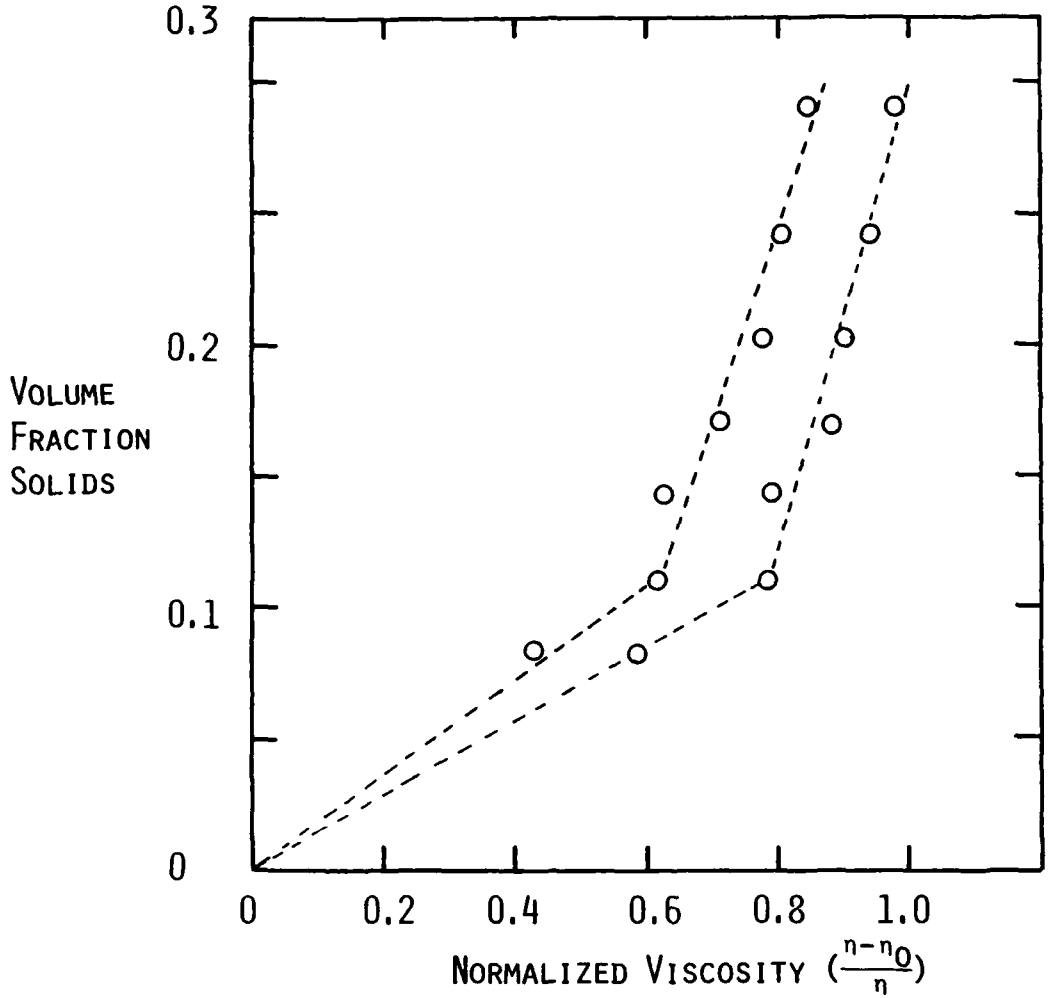
0.3
0.2
0.1
0
VOLUME
FRACTION
SOLIDS
0
0.2
0.4
0.6
0.8
1.0
NORMALIZED VISCOSITY $(\frac{\eta-\eta_0}{\eta})$

Figure 4.

Table 3. Values of $x_v^\infty$ and $k_3$ for PZT slurries.

| Shear Rate ($sec^{-1}$) | $x_v^\infty$ Vol. Fract. PZT | $k_3$ | $r^2$ | $x_v^\infty$ wt% PZT |
|---|---|---|---|---|
| 0.465 | .7952 | -.5377 | .902 | 96.88 |
| 0.950 | .7229 | -.4576 | .926 | 95.43 |
| 2.33 | .6488 | -.3709 | .956 | 93.66 |
| 4.65 | .6000 | -.3097 | .975 | 92.31 |
| 9.30 | .5619 | -.2557 | .988 | 91.12 |
| 18.6 | .5302 | -.2037 | .987 | 90.03 |
| 46.5 | .4951 | -.1334 | .939 | 88.69 |
| 93.0 | insufficient data | | | |

here is appropriate to the doctor blade process, since in both cases the shear rate is developed over small distances.

The $x_v^\infty$ values of Table 3 seem reasonable, but may not have rigorous practical meaning. When these values are plotted as a function of shear rate as in Figure 5, it can be seen that the maximum theoretical solid content decreases with increasing shear rate. This behavior is in conflict with the work of Sikdar and Ore[3] who show a linearly increasing $x_v^\infty$ value with increasing shear rate for calcium sulfate slurries in phosphoric acid.

The discrepancies between our data and the literature on rheology of other slurry systems are only mildly disturbing since the equations are still predictive over the useful range of composition. The differences are perhaps due to the complex nature of the Cladan binder system, or due to size and shape differences between PZT and the $CaSO_4$ particles.

## 2.4 Dependence of Slip Viscosity on Temperature

Another variable that will affect the slip viscosity is temperature. Immediately after ball milling the slip can be quite warm, and depending upon the time before casting the slip may not have reached room temperature. The temperature dependence of the slurry viscosity should be controlled by the rheology of the liquid component. Its dependence can be expressed by[3]

$$\eta_o = k_4 \exp (E/RT) \qquad (9)$$

where E is the activation energy, $k_4$ a proportionality constant and T is absolute temperature. On this basis, we would expect the viscosity to drop with increasing temperature. Table 4 shows two different 70 wt% PZT slips (reprocessed powder) measured at 20 and 25°C on the Brookfield viscometer. The variation in viscosity from slip to slip is greater than the effect of a 5°C change in temperature. In the case of slip H-25, the viscosity measured

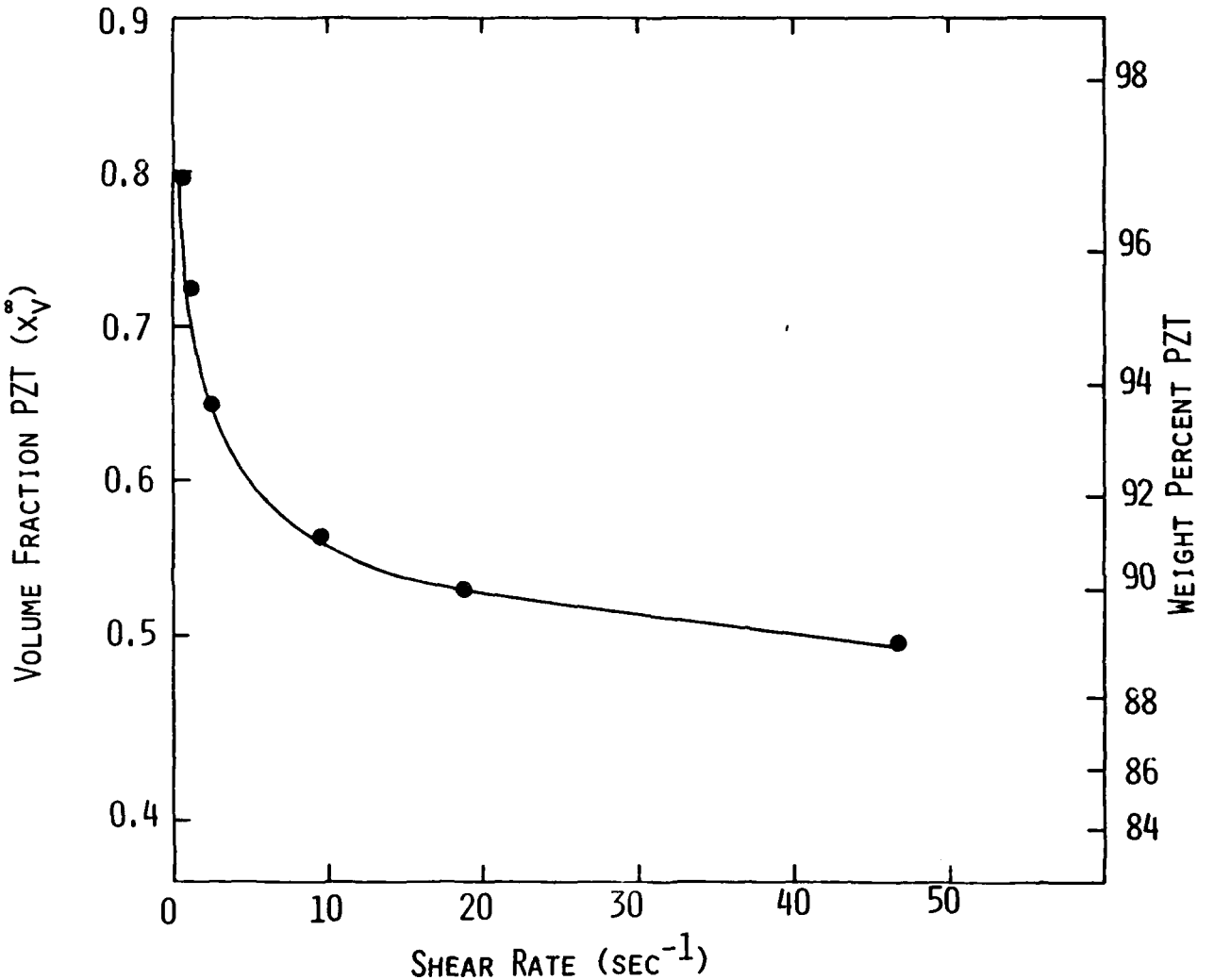
0.9
0.8
0.7
0.6
0.5
0.4
VOLUME FRACTION PZT ($x_V^\infty$)
98
96
94
92
90
88
86
84
WEIGHT PERCENT PZT
0
10
20
30
40
50
SHEAR RATE ($SEC^{-1}$)

Figure 5.

Table 4. Brookfield viscosity of 70 wt% reprocessed-powder slips at 20 and 25°C.

| | Shear Rate ($sec^{-1}$) | Brookfield Viscosity (cP) 20°C | 25°C |
|---|---|---|---|
| H-25 (70w/o PZT) | 0.465 | 9000 | 9350 |
| | 0.950 | 6750 | 6400 |
| | 2.33 | 3850 | 3305 |
| | 4.65 | 2625 | 2375 |
| | 9.30 | 2000 | 1812 |
| | 18.6 | 1623 | 1478 |
| | 46.5 | -- | -- |
| H-43 (70w/o PZT) | 0.465 | 8500 | 12500 |
| | 0.950 | 6000 | 7125 |
| | 2.33 | 3075 | 3750 |
| | 4.65 | 1975 | 2300 |
| | 9.30 | 1312 | 1490 |
| | 18.6 | 942 | 1020 |
| | 46.5 | 745 | 785 |

higher at the higher temperature. These results indicate that the temperature coefficient of viscosity is small in this range, at least compared to our batch-to-batch variations. Alternatively, there may be shortcomings in our measurement technique. It is impossible to completely seal the viscosity chamber during measurement. One possible explanation of the slip H-43 behavior is volatile loss during measurement. This loss would be enhanced by an increase in temperature. If this is the case, then the actual temperature-thinning dependence may be masked in both cases. One alternative that has not yet been investigated is the use of a low density, immiscible, low viscosity surface-fluid (oil or water) to protect the slip during measurement.

According to Cladan, Inc., binder CB73115 is being withdrawn from production because of problems with a hydrophyllic component. Its replacement with equivalent CB73140 may make water an attractive protective fluid for slip viscosity and also for unsealed casting heads.

## 2.5 Viscosity at High Shear Rates and Measurement Calibration

For the same two slips (H-25 and H-43), the viscosity was also measured on the Haake Rotovisco unit. This device measures viscosity continuously over a much wider shear rate range than the Brookfield. Figures 6 and 7 show Brookfield and Haake viscosities for 70 wt% PZT slips H-225 and H-43. The Haake unit (Rotovisco RV-3 with MK 500 measuring head and MV II sensor system) begins to be sensitive above about 50 rpm ($\dot{\gamma}$ = 45 $sec^{-1}$) and continues to about 350 (315 $sec^{-1}$). In this respect, the Haake complements the capability of the Brookfield which ceases to measure tape casting viscosities at about 45 $sec^{-1}$, at least as both our units are now set up.

The Haake and the Brookfield instruments agree fairly well except in the case of the 20°C, H-25 slip measurement and the Haake shows the same inverted temperature dependence for H-43. (Both instruments measure viscosity with the

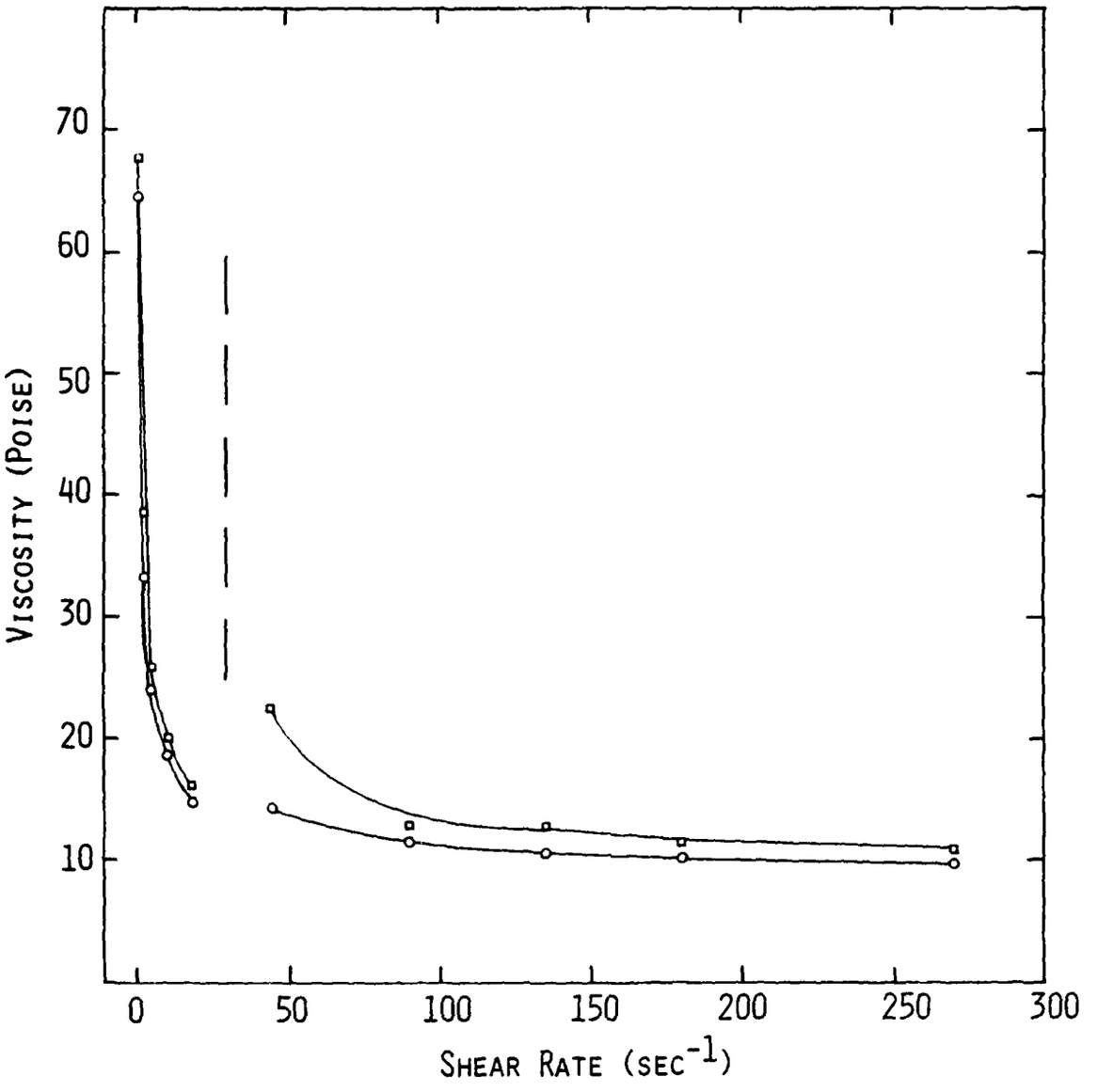
70
60
50
40
30
20
10
VISCOSITY (POISE)
0
50
100
150
200
250
300
SHEAR RATE (SEC$^{-1}$)

Figure 6.

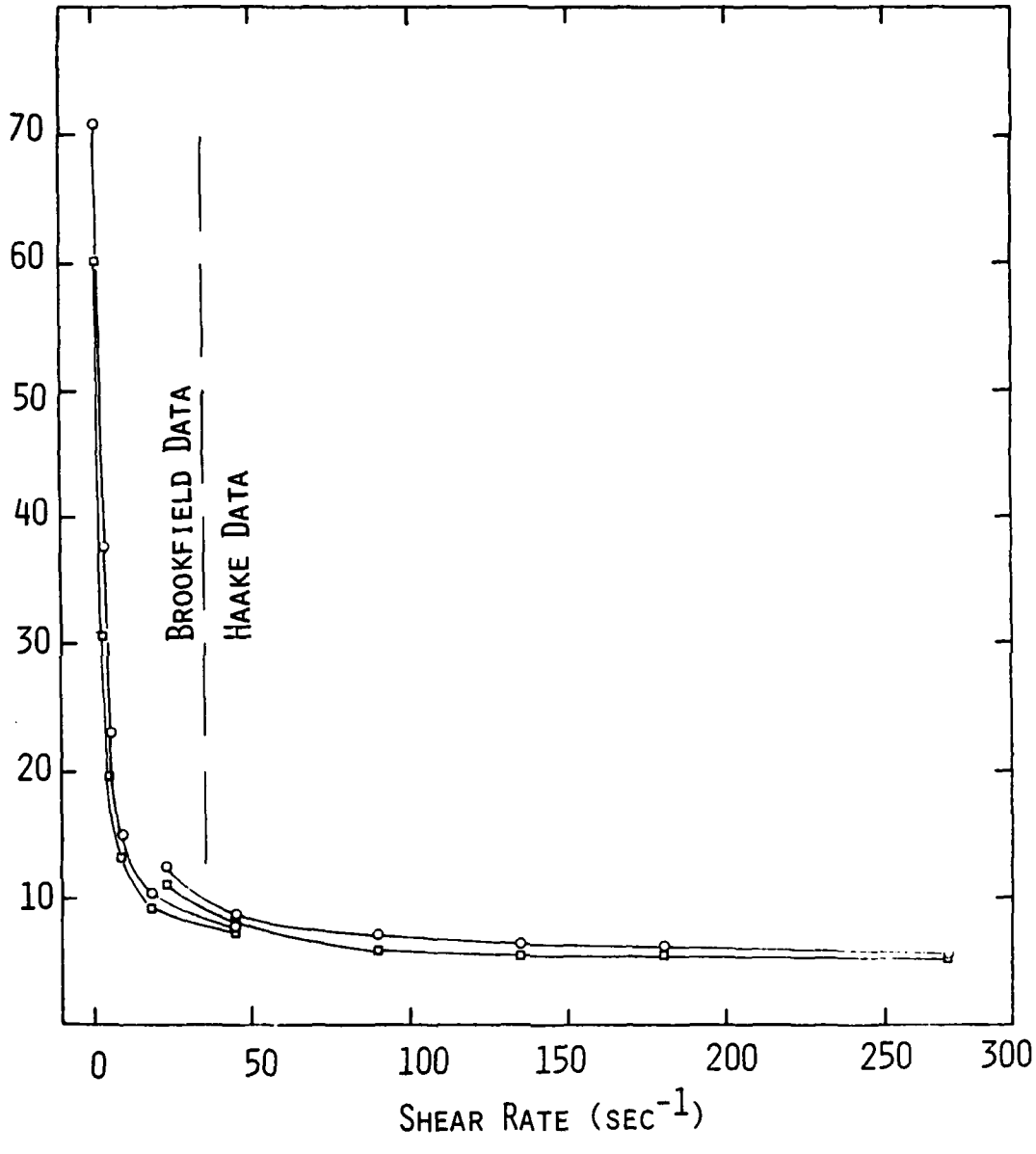
70
60
50
40
30
20
10
0
50
100
150
200
250
300
BROOKFIELD DATA
HAAKE DATA
SHEAR RATE (SEC$^{-1}$)

Figure 7.

sample open to the air.) The general nature of the curve shows that the viscosity is less dependent on the shear rate of measurement at high shear rates. If one were only interested in determining differences in slip rheology at a single shear rate, then a high shear rate measurement might be best.

We should also be interested in measuring rheology at the shear rate of casting operation. This means that disregarding other factors such as mechanical stability of the system, control of the casting operation and the blade height required to produce a desired tape thickness, it would be best to operate the caster at speeds great enough so that small changes in speed do not affect the slip viscosity appreciably.

## 2.6 Shear Rate During Casting

A simple formula may be used to calculate the shear rate developed in the liquid beneath the doctor blade.

The viscosity of a fluid moving under laminar flow is given by

$$\eta = \tau/\dot{\gamma}$$

where $\eta$ is the viscosity in Poise, $\tau$ the shear stress in dynes/cm$^2$, and $\dot{\gamma}$ the shear rate in reciprocal seconds. The shear rate in the case of laminar flow is simply dv/dx, the change in flow rate with distance. For tape casting, this may be determined from $\dot{\gamma}$ = carrier speed/doctor blade height. Table 5 lists shear rates for a variety of blade height-casting speed combinations. This shows that the shear rate during casting of a typical lot of tape prepared for Honeywell Ceramics Center (30 mil blade, 40 in/min) is 16.7 sec$^{-1}$. This value is near the maximum shear rate measureable using our Brookfield viscometer for a typical slip with 70 wt% powder. The measured viscosity at this shear rate is near 2000 cPs as shown in Table 1.

Table 5. Shear rate in casting at various blade heights and carrier velocities.

| Casting Speed (in/min) | Blade Height (mils) | | | | | | |
|---|---|---|---|---|---|---|---|
| | 2 | 5 | 10 | 15 | 20 | 30 | 40 |
| 10 | 83.3 | 33.3 | 16.7 | 11.1 | 8.33 | 5.56 | 4.17 |
| 20 | 166 | 66.7 | 33.3 | 22.2 | 16.7 | 11.1 | 8.33 |
| 30 | 250 | 100 | 50.0 | 33.3 | 25.0 | 16.7 | 12.5 |
| 40 | 333 | 133 | 66.7 | 44.4 | 33.3 | 22.2 | 16.7 |
| 50 | 417 | 167 | 83.3 | 55.6 | 41.7 | 27.8 | 20.8 |
| 60 | 500 | 200 | 100 | 66.7 | 50.0 | 33.3 | 25.0 |
| 70 | 583 | 233 | 117 | 77.8 | 58.3 | 38.9 | 29.2 |
| 80 | 667 | 267 | 133 | 88.9 | 66.7 | 44.4 | 33.3 |
| 90 | 750 | 300 | 150 | 100 | 75 | 50 | 37.5 |
| 100 | 833 | 333 | 167 | 111 | 83.3 | 55.6 | 41.7 |
| 120 | 1000 | 400 | 200 | 133 | 100 | 66.7 | 50.0 |
| 140 | 1167 | 467 | 233 | 156 | 117 | 77.8 | 58.3 |
| 160 | 1333 | 533 | 267 | 178 | 133 | 88.9 | 66.7 |
| 180 | 1500 | 600 | 300 | 200 | 150 | 100 | 75.0 |

## 3.0 Tape Casting of As-Received Powder

The following section summarizes the physical data collected subsequent to tape casting of the slurries described in Section 2.0. Tape was cast at various doctor blade heights using the double blade casting head described in earlier reports. Carrier velocity was 40 $\pm$ 2 in/min throughout this study unless otherwise noted. Since the blade heights used were generally high compared to normal operation, the tape was allowed to dry for 5-10 minutes prior to removal from the casting machine to prevent slosh of the slurry. After 10 to 20 minutes, the tape was stripped from the carrier, cut into 8-10 inch lengths placed on paper and stacked. After one to two days further drying, the tape was stored in a sealed bag.

One inch squares were 'shear punched' (see earlier reports) from the tape. Random squares were used in tape thickness and geometric density measurements. Squares were assembled in 10 to 20 layer stacks and laminated in a square press die in a heated press. Lamination was carried out at 5000 psi, 55° $\pm$ 3°C for 60 seconds. Early work included duplicate samples laminated under ambient pressure and under low-vacuum. In the case of vacuum laminations, vacuum was applied 1-2 min. prior to the onset of ram pressure.

After taking laminate weight and dimensional measurements (and in some cases immersion density), the samples were burned out using the cycle described in Report I. Samples were then fired in closed $Al_2O_3$ crucibles at 1275°C for 1/2 hour with $PbZrO_3$ as a lead source. Subsequently, final density and dimensions of the samples were determined. The study did not proceed to the point of taking electrical data since these measurements were being performed at Honeywell Ceramics Center on scaled-up devices that used both MRL and HCC tape.

### 3.1 Thickness Measurements and Shrinkage

Table 6 lists tape thickness and laminate layer thickness for ambient and vacuum laminated stacks before and after firing for slurries with various solids loadings. Shrinkage on drying, lamination and firing is also calculated.

Both the green tape thickness and the fired layer thickness are directly related to the doctor blade height, as one might expect. As shown in Figure 8 however, the data becomes more irregular at larger blade heights. This may be because at greater blade heights, the tape thickness may be more dependent upon how the slurry spreads and sets after casting.

Also important is the dependence of tape thickness and fired layer thickness on solids loading of the slurry (Figure 9) since this points out that small variations in batching or uncontrolled loss of solvents during milling or casting may affect the dimensional uniformity of the tape and the fired multilayer. An important slurry measurement prior to casting is the pycnometer density since this can point out compositional variations and can also be used to calculate adjustments.

### 3.2 Density Measurements

The density of tape and green and fired laminates is collected in Table 7. The doctor blade setting has no apparent effect on the density at any stage in the process. The effect of solids loading is shown in Figure 10. As the binder content is decreased, the green density of the tape rises pretty much uniformly but does not exceed 4.0 $gm/cm^3$ until the solids loading reaches 75 wt%. These values are somewhat low compared to earlier work on tape-cast PZT wherein a value of 4.0 was considered minimum tape density to achieve good fired density for 70 weight percent solids slurries. This indicates that in

Table 6. Thickness measurements of tape and green and fired laminates prepared from as-received powder.

| Slip No. | Solids Content Wt% | Solids Content Vol% | Blade (mils) | Tape ± σ mils | Laminate Amb. | Laminate Vac. | Fired Stack Amb. | Fired Stack Vac. | % Shrinkage (mean) Drying* | Lam.* | Fire* | Total* |
|---|---|---|---|---|---|---|---|---|---|---|---|---|
| H-10 | 75.00 | 29.20 | 20 | 8.76±0.31 | 7.12 | -- | 6.27 | -- | 56.2 | 18.7 | 28.4 | 68.7 |
| | | | 25 | 11.83±0.74 | 9.57 | -- | 8.03 | -- | 52.7 | 19.1 | 32.1 | 73.2 |
| | | | 30 | 14.01±0.42 | -- | -- | -- | -- | 53.3 | -- | -- | -- |
| | | | | | | | | Mean: | (54.1) | (18.9) | (30.3) | (71.0) |
| H-15 | 69.93 | 24.23 | 20 | 8.52±0.22 | 6.61 | 6.82 | 5.65 | 5.75 | 57.4 | 21.2 | 33.2 | 71.5 |
| | | | 25 | 11.12±0.51 | 9.11 | 9.06 | 7.59 | 7.60 | 55.5 | 18.3 | 31.7 | 69.6 |
| | | | 30 | 12.39±0.25 | 10.07 | 11.53 | 8.49 | 9.53 | 58.7 | 12.8 | 27.3 | 70.0 |
| | | | | | | | | Mean: | (57.2) | (17.4) | (30.7) | (70.4) |
| H-11 | 65.00 | 20.34 | 20 | 7.24±0.41 | 5.75 | 5.81 | 4.87 | 5.01 | 63.8 | 20.2 | 33.4 | 75.3 |
| | | | 25 | 9.30±0.55 | 8.01 | 7.44 | 6.65 | 6.11 | 62.8 | 16.9 | 31.4 | 74.5 |
| | | | 30 | 12.64±0.67 | 10.33 | 10.65 | 8.63 | 8.71 | 57.9 | 17.0 | 31.4 | 71.1 |
| | | | | | | | | Mean: | (61.5) | (18.0) | (32.1) | (73.6) |
| H-16 | 60.00 | 17.10 | 20 | 6.65±0.21 | 5.52 | 5.78 | 4.50 | 4.57 | 66.8 | 15.0 | 31.8 | 77.3 |
| | | | 25 | 8.89±0.24 | 7.61 | 7.70 | 6.21 | 6.08 | 64.4 | 13.9 | 30.9 | 75.4 |
| | | | 30 | 11.18±0.68 | 9.56 | 9.28 | 7.82 | 7.46 | 62.7 | 20.2 | 31.7 | 74.5 |
| | | | | | | | | Mean: | (64.6) | (16.4) | (31.5) | (75.7) |
| H-7 | 55.00 | 14.39 | 20 | 6.51±0.21 | 4.42 | -- | -- | -- | 67.5 | 32.1 | -- | -- |
| H-8 | 50.00 | 12.09 | 15 | 3.79±0.17 | 2.85 | -- | 2.38 | -- | 74.7 | 24.8 | 37.2 | 84.1 |
| H-9 | 40.00 | 8.40 | 10 | 2.58±0.23 | -- | -- | -- | -- | 74.2 | -- | -- | -- |
| | | | | | | | | | *re: blade | *re: tape | *re: tape | *re: blade |

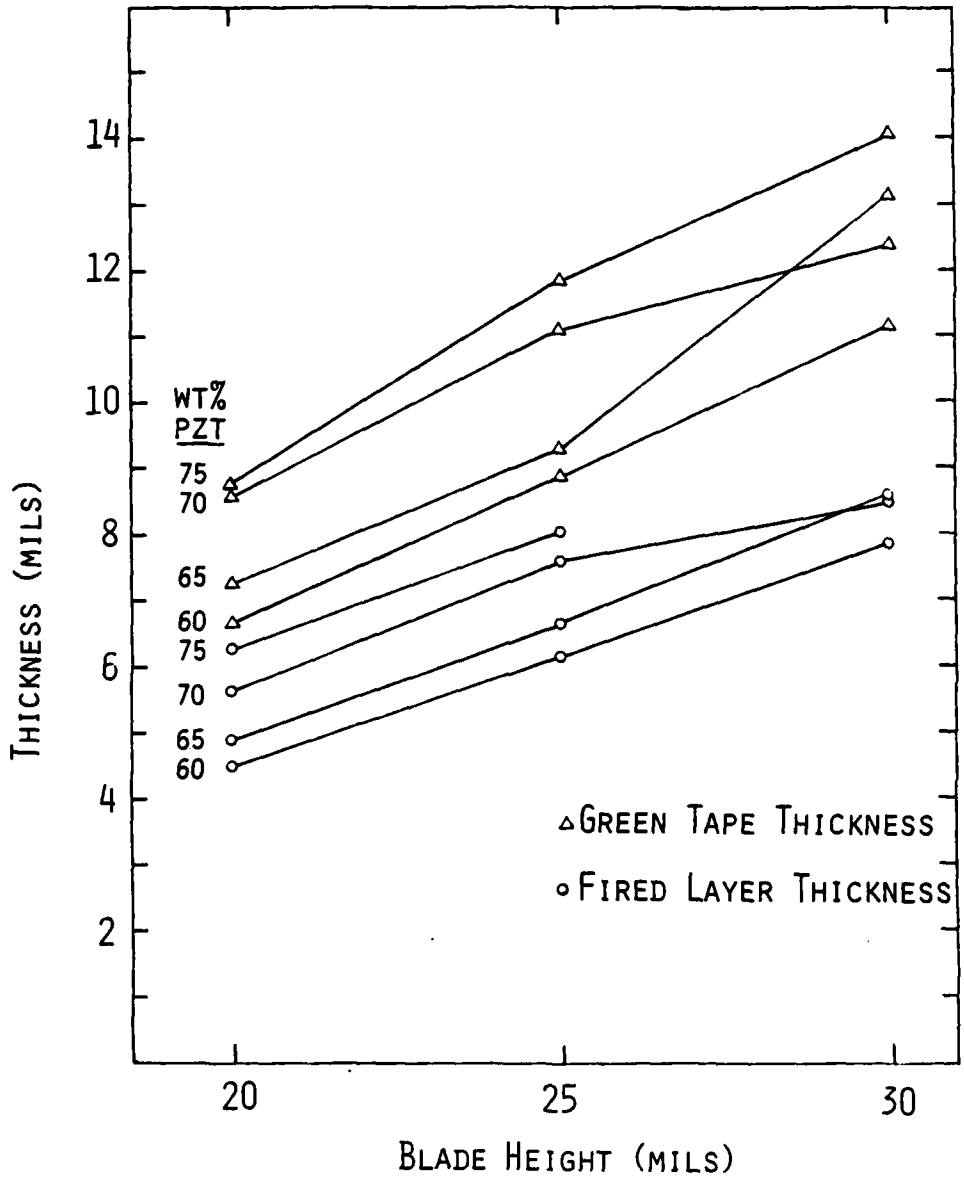
14
12
10
8
6
4
2
THICKNESS (MILS)
WT%
PZT
75
70
65
60
75
70
65
60
△GREEN TAPE THICKNESS
○FIRED LAYER THICKNESS
20
25
30
BLADE HEIGHT (MILS)

Figure 8.

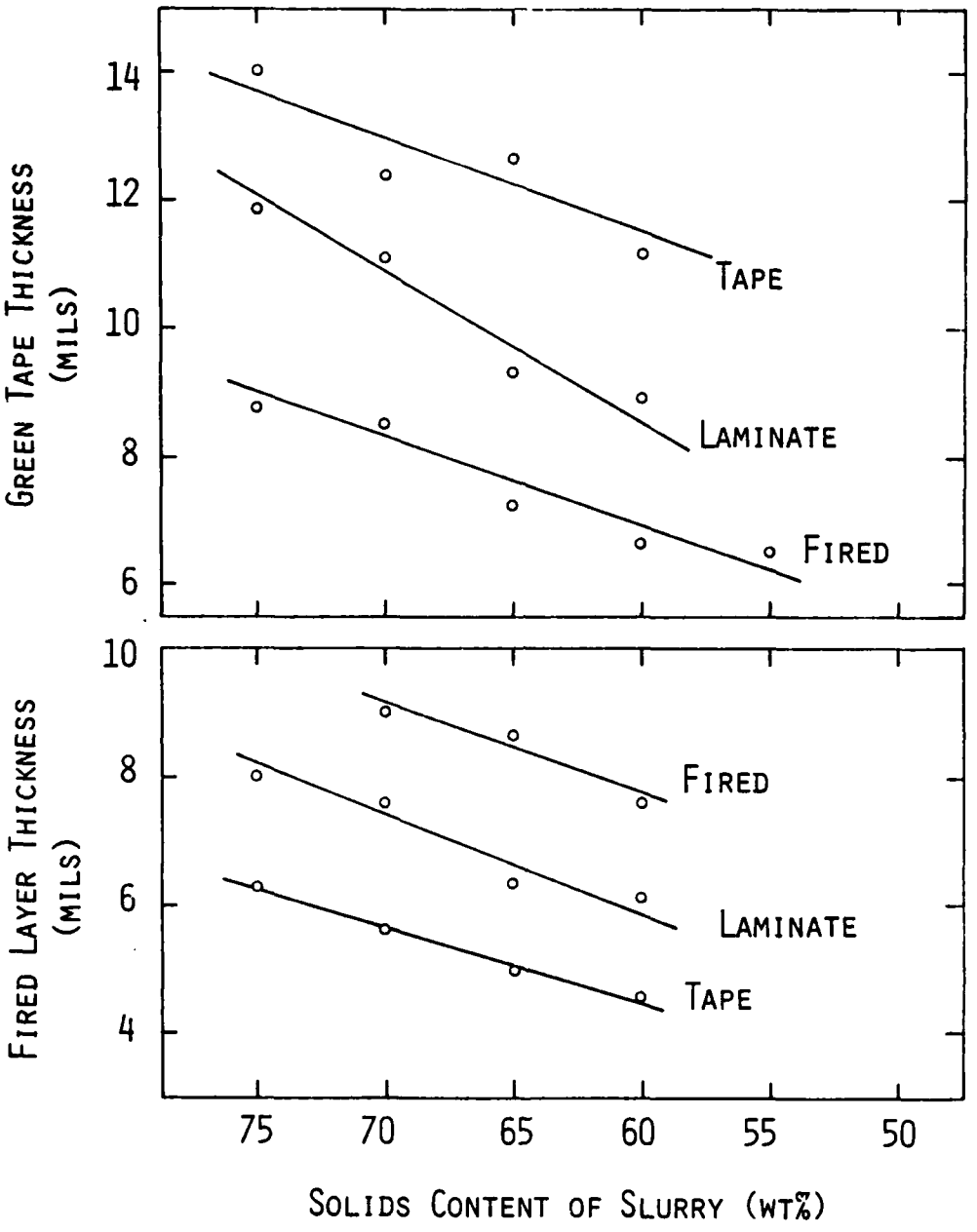
GREEN TAPE THICKNESS (MILS)
14
12
10
8
6
TAPE
LAMINATE
FIRED
FIRED LAYER THICKNESS (MILS)
10
8
6
4
FIRED
LAMINATE
TAPE
75
70
65
60
55
50
SOLIDS CONTENT OF SLURRY (WT%)

Figure 9.

Table 7. Density measurements of tape, and green and fired laminates prepared from as-received powder.

| Slip No. | Binder Content Wt% | Vol% | Blade (mils) | Tape g/cc ± σ | Laminates Amb. | Vac. | Fired (immerse) Amb. | Vac. | % Theo. Amb. | Vac. |
|---|---|---|---|---|---|---|---|---|---|---|
| H-10 | 25.00 | 70.80 | 20 | 4.08±0.14 | 4.73 | 4.67 | 7.57 | 7.44 | 94.6 | 93.0 |
| | | | 25 | 3.99±0.25 | 4.62 | -- | 7.42 | -- | 92.8 | -- |
| | | | 30 | 4.02±0.12 | -- | -- | -- | -- | -- | -- |
| H-15 | 30.07 | 75.77 | 20 | 3.81±0.20 | 4.85 | 4.67 | 7.48 | 7.46 | 93.5 | 93.3 |
| | | | 25 | 3.78±0.07 | 4.62 | 4.68 | 7.48 | 7.17 | 93.5 | 89.6 |
| | | | 30 | 3.84±0.30 | 4.47 | 4.67 | 7.50 | 7.45 | 93.8 | 93.1 |
| H-11 | 35.00 | 79.66 | 20 | 3.76±0.36 | 4.55 | 4.60 | 7.10 | 7.53 | 88.8 | 94.1 |
| | | | 25 | 3.76±0.22 | 4.40 | 4.49 | 7.05 | 7.49 | 88.1 | 93.6 |
| | | | 30 | 3.81±0.20 | 4.42 | 4.56 | 7.10 | 7.55 | 88.8 | 94.4 |
| H-16 | 40.00 | 82.90 | 20 | 3.56±0.21 | 4.15 | 4.15 | 6.75 | 7.30 | 84.4 | 91.3 |
| | | | 25 | 3.67±0.18 | 4.16 | 4.16 | 6.68 | 7.23 | 83.5 | 90.4 |
| | | | 30 | 3.67±0.17 | 4.24 | 4.28 | 6.70 | 7.27 | 83.8 | 90.9 |
| H-7 | 45.00 | 85.61 | 20 | 3.48±0.11 | 3.79 | -- | -- | -- | | |
| H-8 | 50.00 | 87.91 | 15 | 3.34±0.15 | 3.69 | -- | 6.30 | -- | | |
| H-9 | 60.00 | 91.60 | 10 | 2.98±0.27 | -- | -- | -- | -- | | |

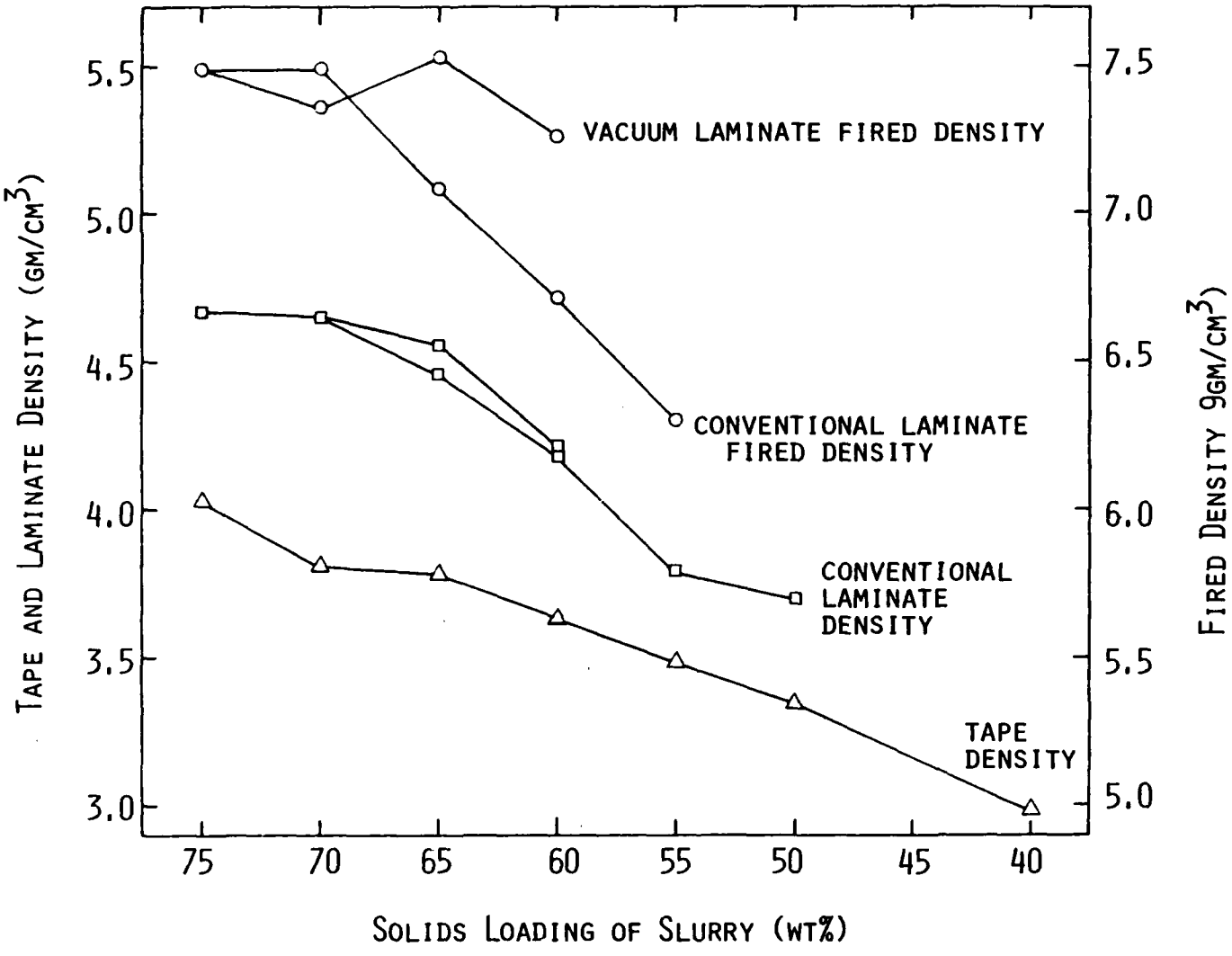
VACUUM LAMINATE FIRED DENSITY
CONVENTIONAL LAMINATE FIRED DENSITY
CONVENTIONAL LAMINATE DENSITY
TAPE DENSITY
TAPE AND LAMINATE DENSITY (GM/CM3)
FIRED DENSITY 9GM/CM3)
SOLIDS LOADING OF SLURRY (WT%)
5.5
5.0
4.5
4.0
3.5
3.0
7.5
7.0
6.5
6.0
5.5
5.0
75
70
65
60
55
50
45
40

Figure 10.

the present case the grain size distribution maybe less favorable to achieving good particle packing in the tape than in earlier work.

This conclusion is supported by the fired density curve. The final density is maximized at a solids loading of about 70%. Further increasing the solids:binder ratio in the slurry does not further increase the fired density indicating that particle packing constraints become operative at the 70% solids level.

The laminate density is significantly greater than the tape density. The Cladan CB73115 is a medium porosity binder that dries and burns-out well compared to some of the denser systems. Much of the porosity inherent in the green tape collapses during the lamination step. The use of vacuum during lamination gives only a small improvement of the green laminate density, as may be expected if small amounts of interlaminar porosity were removed. The effect on fired density is more difficult to understand. The data is not well balanced, but it appears that vacuum during lamination enhances the density only if excess binder is present. This may be due to enhanced removal of volatile binder phases or trapped solvent under vacuum.

### 3.3 Weight Loss Measurements

Weight loss on firing may be used to determine the binder content of the dried tape. Fired weight loss of laminates prepared from as-received powder is summarized in Table 8. If we assume there is negligible weight loss during lamination, then the weight loss on firing is equal to the binder content. This allows us to calculate the percentages of the Cladan binder composition that remains after drying. Averaging the results of this calculation for each of the slips gives a value of 20.07 weight percent solids relative to the binder liquid.

Table 8. Weight loss on firing for samples prepared from as-received powder.

| Slip | wt% Solids | % wt loss on Firing | N | wt% binder in CB73115* |
|---|---|---|---|---|
| H-10 | 75.0 | 6.37±.91 | 2 | 20.41 |
| H-15 | 69.9 | 8.25±.13 | 5 | 20.88 |
| H-11 | 65.0 | 9.70±.20 | 6 | 19.95 |
| H-16 | 60.0 | 11.50±.26 | 5 | 19.49 |
| H-8 | 50.0 | 16.42- | 1 | 19.64 |
| | | | mean: | 20.07±.57 |

*after drying.

## 3.4 Typical Physical Properties

Using data from the preceding section and assuming the density of PZT is 8.0, and the density of the binder is 1.1, the weight and volume composition and composite density can be calculated for various stages in the tape casting process (see Table 9). It is interesting to note that for a 70 wt% solids slurry, 75.7 percent of the volume is binder. In the dried tape there is 25% porosity by volume and the volume fraction binder is still very large. On lamination much of the porosity collapses, but only 53.5 percent of the volume is actual PZT powder. This condition remains after burn-out since if the burn-out is conducted properly, there should be little or no binder flow leading to particle rearrangement. Thus, the sample enters the firing stage at about 54% of theoretical density.

It is probably true that the rather large amount of tape porosity associated with this binder is not necessarily disadvantageous. The porosity in the laminate probably represents a stable value based on the packing factor of the powder and the use of a more densely drying binder may not improve the density of the burned-out laminate. Some porosity in the laminate is helpful during the burn-out cycle. Binders that dry to high density are more durable in subsequent handling, but also more difficult to remove from the carrier.

## 4.0 Comparison of As-Received and Reprocessed Powder

The somewhat poor green density of the tape prepared with as-received powder and the achievement of fired densities below 95% of theoretical, led us to suspect that agglomerates present in the powder were preventing good particle packing. Initial attempts at screening through 325 mesh gave poor yields so the powder was dried at 300°C and dry ball milled. It then was sieved through 325 mesh with the aid of small $ZrO_2$ media placed in the powder to break up cakes.

Table 9. Typical composition and density at various stages in the multilayer process for PZT. (HCC as-received powder)

| | wt% PZT | wt% Binder | Vol% PZT | Vol% Binder | Vol% Porosity | Meas Density | Theo Density |
|---|---|---|---|---|---|---|---|
| Slurry | 70.0 | 30.0 | 24.3 | 75.7 | — | -- | 2.8 |
| Tape | 91.7 | 8.3 | 43.3 | 31.2 | 25.5 | 3.8 | 5.1 |
| Lam | 91.7 | 8.3 | 53.5 | 38.6 | 7.9 | 4.7 | 5.1 |
| Burn-Out | 100.0 | 0.0 | 53.5 | 0.0 | 46.5 | -- | 8.0 |
| Fired | 100.0 | 0.0 | 0.0 | 0.0 | 6.3 | 7.5 | 8.0 |

## 4.1 Powder Characteristics

The agglomerate size and shape distribution was determined using a computer beam controlled SEM* technique[1], and the specific surface of the powder was evaluated by BET[2] analyses**. The results are shown in Table 10 for both the as-received and reprocessed powders. In both cases the change was small, but in the predicted direction. The agglomerate size was slightly smaller and the surface area slightly larger for the reprocessed powder. The agglomerate shape ratio indicates that agglomerates were slightly more elongate in the reprocessed powder. The particle size and shape distributions are shown in Figures 11 through 14 and again are very similar in nature.

## 4.2 Pellet Study

In order to determine the effectiveness of reprocessing the powder and to determine the proper firing temperature, a pellet study was conducted. Pellets were pressed from as-received and reprocessed powder with three wt% PVA binder and fired in groups of six, three from each powder type. Since the HCC powder was described as a hard PZT, temperatures were chosen from the lower, soft PZT firing temperature (1285°C at MRL) to the hard PZT firing temperature (1330°C). Weight loss corrected for binder content was determined. Results appear in Table 11. Green and fired density of the reprocessed powder is consistently higher and the weight loss is consistently lower. Immersion density was performed when it was considered that the geometric density consistently gave a low estimate. Results indicate that the reprocessed powder pellets are slightly better than the as-received. The firing study indicates that the sample density was greatest at 1285°C.

---

*D.E.C., Inc. PDP 11/20 Computer with JEOL Ltd., JSM 50-A SEM.
**Quantachrome, Inc., Monosorb Model MS-4.

Table 10. Honeywell PZT powder characteristics.

| Powder | BET Analysis | | | SEM Agglomerate Size and Shape | | |
|---|---|---|---|---|---|---|
| | $S_m$[1] $m^2/gm$ | D[2] (μm) | No. Meas. | Mean Size (μm) | Diam. Ratio min/max | No. Particles |
| As Received | 0.66 | 1.14 | 4 | 4.20±2.5 | 0.51±0.17 | 1015 |
| Reprocessed[3] | 0.87 | 0.86 | 3 | 3.96±2.9 | 0.46±0.17 | 1008 |

(1) Surface area per unit mass of powder.
(2) Calculated BET equivalent spherical particle size: D (μm) = 6/Sm ($m^2/gm$) x ρ($gm/cm^3$).
(3) 24 hour dry mill ($ZrO_2$ media), 325 mesh sieving.

Figure 11. Agglomerate average diameter distribution for as-received Honeywell PZT powder (Batch 4516B).

CLASS PERCENT

| | Upper Class Limit | 0 1 2 3 4 5 | Class % | Particle Count |
|---|---|---|---|---|
| | 0.25 | [ | 0.00 | 0 |
| | 0.40 | [ | 0.10 | 1 |
| M | 0.63 | [ | 0.89 | 9 |
| I | 1.00 | [* * | 3.74 | 38 |
| C | 1.60 | [* * * * | 7.49 | 76 |
| R | 2.50 | [* * * * * * * * | 16.06 | 163 |
| O | 4.00 | [* * * * * * * * * * * * | 25.22 | 256 |
| N | 6.30 | [* * * * * * * * * * * * * * * | 30.44 | 309 |
| S | 10.00 | [* * * * * * | 12.61 | 128 |
| | 16.00 | [* * | 3.35 | 34 |
| | 25.00 | [ | 00.10 | 1 |

Mean Diameter: 4.20 μm, Standard Deviation: 2.5 μm, Particle Count: 1015.

Figure 12. Agglomerate minimum/maximum diameter distribution for as-received Honeywell PZT powder (Batch 4516B).

CLASS PERCENT

| | Upper Class Limit | 0 1 2 3 | Class % | Particle Count |
|---|---|---|---|---|
| | 0.050 | [ | 0.30 | 3 |
| | 0.100 | [* | 1.08 | 11 |
| | 0.150 | [* | 1.87 | 19 |
| | 0.200 | [* | 2.27 | 23 |
| | 0.250 | [* | 2.96 | 30 |
| | 0.300 | [* * | 3.94 | 40 |
| | 0.350 | [* * * | 5.81 | 59 |
| R | 0.400 | [* * * | 7.00 | 71 |
| A | 0.450 | [* * * * | 8.77 | 89 |
| T | 0.500 | [* * * * * | 10.05 | 102 |
| I | 0.550 | [* * * * * * | 12.32 | 125 |
| O | 0.600 | [* * * * * * | 11.92 | 121 |
| | 0.650 | [* * * * * | 9.06 | 92 |
| | 0.700 | [* * * * | 8.37 | 85 |
| | 0.750 | [* * * * | 7.49 | 76 |
| | 0.800 | [* * | 4.14 | 42 |
| | 0.850 | [* | 1.87 | 19 |
| | 0.900 | [ | 0.69 | 7 |
| | 0.950 | [ | 0.10 | 1 |

Mean: 0.51, Standard Deviation: 0.17, Particle Count: 1015.

Figure 13. Agglomerate average diameter distribution for reprocessed Honeywell PZT powder (Batch 4516B).

CLASS PERCENT

| | Upper Class Limit | 0 1 2 3 4 5 | Class % | Particle Count |
|---|---|---|---|---|
| | 0.25 | [ | 0.00 | 0 |
| | 0.40 | [ | 0.10 | 1 |
| M | 0.63 | [* | 1.49 | 15 |
| I | 1.00 | [* * * | 5.26 | 53 |
| C | 1.60 | [* * * * * | 10.91 | 110 |
| R | 2.50 | [* * * * * * * | 14.58 | 147 |
| O | 4.00 | [* * * * * * * * * * * * | 24.70 | 249 |
| N | 6.30 | [* * * * * * * * * * * * * * * | 29.76 | 300 |
| S | 10.00 | [* * * * * | 10.52 | 106 |
| | 16.00 | [* | 1.98 | 20 |
| | 25.00 | [ | 0.40 | 4 |
| | 40.00 | [ | 0.30 | 3 |

Mean Diameter: 3.96 μm, Standard Deviation: 2.9 μm, Particle Count: 1008.

Figure 14. Agglomerate minimum/maximum diameter distribution for reprocessed Honeywell PZT powder (Batch 4561B).

CLASS PERCENT

| | Upper Class Limit | 0 1 2 3 | Class % | Particle Count |
|---|---|---|---|---|
| | 0.050 | [ | 0.60 | 6 |
| | 0.100 | [* | 1.19 | 12 |
| | 0.150 | [* | 1.39 | 14 |
| | 0.200 | [* | 2.80 | 29 |
| | 0.250 | [* * * | 5.46 | 55 |
| | 0.300 | [* * * | 5.75 | 58 |
| | 0.350 | [* * * * | 7.64 | 77 |
| R | 0.400 | [* * * * * | 10.22 | 103 |
| A | 0.450 | [* * * * * | 10.42 | 105 |
| T | 0.500 | [* * * * * * | 12.60 | 127 |
| I | 0.550 | [* * * * * * | 11.71 | 118 |
| O | 0.600 | [* * * * | 8.04 | 81 |
| | 0.650 | [* * * * | 7.74 | 78 |
| | 0.700 | [* * * | 6.65 | 67 |
| | 0.750 | [* * * | 5.06 | 51 |
| | 0.800 | [* | 1.39 | 14 |
| | 0.850 | [ | 0.99 | 10 |
| | 0.900 | [ | 0.30 | 3 |
| | 0.950 | [ | 0.00 | 0 |

Mean: 0.46, Standard Deviation: 0.71, Particle Count: 1008.

Table 11. Denisty and weight loss of pellets of as-received and reprocessed powder.

| Powder Type | Firing Temp (°C) | Geometric Density | | | | Immersion Density | | Weight Loss (%) |
|---|---|---|---|---|---|---|---|---|
| | | Green ($g/cm^3$) | Theo (%) | Fired ($gm/cm^3$) | Theo (%) | Fired ($g/cm^3$) | Theo (%) | |
| As-Rec. | 1285 | 5.13 | 64.1 | 7.33 | 91.6 | 7.58 | 94.8 | 1.35 |
| As-Rec. | 1300 | 5.21 | 65.1 | 7.40 | 92.5 | 7.61 | 95.1 | 1.37 |
| As-Rec. | 1315 | 5.20 | 65.0 | 7.32 | 91.5 | 7.58 | 94.8 | 1.26 |
| As-Rec. | 1330 | 5.10 | 63.8 | 7.15 | 89.4 | 7.43 | 92.9 | 2.07 |
| Reproc. | 1285 | 5.34 | 66.8 | 7.43 | 92.9 | 7.62 | 95.3 | 0.90 |
| Reproc. | 1300 | 5.33 | 66.6 | 7.42 | 92.8 | 7.60 | 95.0 | 1.05 |
| Reproc. | 1315 | 5.38 | 67.3 | 7.34 | 91.8 | 7.50 | 93.8 | 0.81 |
| Reproc. | 1330 | 5.37 | 67.1 | 7.35 | 91.9 | 7.49 | 93.6 | 1.05 |

Reprocessed powder: Dry ball milled 24 hr. with $ZrO_2$ media, screened -325 mesh.

Pellets: Prepared with 3 wt% PVA binder, pressed on rotary press (pressure unknown); burned out 30 min, 600°C; fired 30 minutes at temp, closed crucible, Pt setter, $PbZrO_3$ source material. 3 pellets/group, all temps simultaneous.

## 4.3 Slurry and Tape Properties

Comparative properties for both powders at various stages in the multilayer fabrication process are shown in Table 12. Slightly smaller agglomerate size and slightly larger surface area are indicative of agglomerate breakdown. The viscosity of a 70 wt% PZT slurry is decreased slightly for reprocessed powder. This is contrary to expectation since the surface area is higher. Normally one would expect the greater surface area to require more liquid to coat the particles leaving less to flow between particles and thus increasing the resistance to shear. The decrease in viscosity may be due to less particle-particle interference because the agglomerates are broken up or rounded off in the milling step.

Reprocessing has led to small but significant increases in the tape and laminate density and the fired density is in the 95% range. Only reprocessed powder will be used in the remainder of the study. The only tape prepared from as-received powder sent to Honeywell Ceramics Center was from slips H-20 and H-21.

## 5.0 Tape Casting of Reprocessed Powder

Reprocessed powder (dry ball milled and sieved -325 mesh) has been prepared as 70 and 75 weight percent solids slurries. Besides using this material for preparation of tape for Honeywell Ceramics Center, studies were designed to ascertain the effect of temperature on slip viscosity (see Section 2.4), the effect of carrier velocity on tape, laminate and fired properties, and to reaffirm the thickness and density results using this powder.

## 5.1 Rheology of Reprocessed-Powder Slurries

The viscosity of reprocessed-powder slurries is shown in Table 13 as average values of increasing and decreasing rpm. All 70 wt% slurries (except H-35 which appears to be anomalous) are averaged for comparison to as-received

Table 12. Effect of powder milling on preparation of PZT multilayers.

| | As-Received | Re-Milled* |
|---|---|---|
| Powder Characteristics | | |
| Agglomerate Size (μm) | 4.20 | 3.96 |
| BET Surface Area ($m^2$/gm) | 0.66 | 0.87 |
| Slurry Viscosity (70 wt% in CB73115, 23°C) | | |
| $\dot{\gamma}$ = 0.95 $sec^{-1}$ (cP) | 7450 | 6500 |
| $\dot{\gamma}$ = 18.6 $sec^{-1}$ (cP) | 2320 | 1960 |
| Tape Geometric Density (cast at 1.78 cm/sec) | | |
| .051 cm blade ($gm/cm^2$) | 3.81 | 4.19 |
| .076 cm blade ($gm/cm^3$) | 3.84 | 4.26 |
| Laminate Geometric Density (5 ksi, 55°C, 60 sec) | | |
| .051 cm blade ($gm/cm^2$) | 4.67 | 4.82 |
| .076 cm blade ($gm/cm^2$) | 4.67 | 4.94 |
| Fired MLT Immersion Density | | |
| .051 cm blade ($gm/cm^3$, % theo.) | 7.41, 92.6 | 7.58, 94.8 |
| .076 cm blade ($gm/cm^3$, % theo.) | 7.30, 91.3 | 7.63, 95.4 |

*Dry ball milled 24 hr, sieved -325 mesh.

Table 13. Viscosity[+] of slurries prepared from reprocessed powder.

| Slurry No. | Wt% Solids | Spindle Rotation (rpm) 0.5 | 1.0 | 2.5 | 5.0 | 10 | 20 | 50 | Temp ±1°C |
|---|---|---|---|---|---|---|---|---|---|
| H-23 | 70.0 | N.R. | N.R. | 4,300 | 3,155 | 2,490 | 2,080 | -- | N.R. |
| H-24 | 70.0 | N.R. | N.R. | 5,600 | 3,800 | 2,690 | 2,140 | -- | N.R. |
| H-32 | 70.0 | 14,500 | 9,100 | 4,600 | 2,900 | 2,100 | 1,630 | -- | 22 |
| H-33 | 70.0 | 10,600 | 6,450 | 3,440 | 2,420 | 1,815 | 1,445 | -- | N.R. |
| H-35 | 69.9 | 31,500 | 16,750 | 7,900 | 4,960 | 3,410 | -- | -- | 22 |
| H-36 | 70.0 | 12,000 | 7,000 | 3,950 | 2,630 | 1,915 | 1,505 | -- | 21 |
| Mean Val.*: | | 12,365 | 7,515 | 4,380 | 2,980 | 2,200 | 1,760 | -- | -- |
| Stnd. Dev.: | | ±1,975 | ±1,400 | ±810 | ±535 | ±375 | ±330 | -- | -- |
| H-13(1) | 70.0 | 12,500 | 7,450 | 4,390 | 3,035 | 2,170 | 1,885 | -- | N.R. |
| H-15(1) | 70.0 | N.R. | N.R. | 5,350 | 3,890 | 2,520 | 2,670 | -- | N.R. |
| H-29 | 75.0 | 21,150 | 12,850 | 7,350 | 5,165 | 3,965 | -- | -- | 23°C |
| H-10(1) | 75.0 | 42,000 | 25,500 | 14,800 | -- | -- | -- | -- | N.R. |

(1) As-received powder slurry for comparison.
*H-35 data not included.
[+]Brookfield Rheolog: RVT-RL, small sample adapter: SC-4 spindle: 21.
N.R. - Not recorded.

slurries H-13 and H-15. The scatter in viscosity data as represented by the standard deviation is fairly consistent at 16 to 19% of the measurement and indicates no particular measurement rpm as being particularly accurate. On the average, the reprocessed powder viscosities appear to be slightly lower than those of the as-received powder.

Only two slurries are available to compare as-received and reprocessed slurry viscosity at 75 wt% solids. The viscosity of the reprocessed powder slurry is roughly 85% that of the as-received powder over the range of comparison.

## 5.2 Thickness and Density of Reprocessed Powder Samples

Thickness and density data for material prepared from reprocessed powder are listed in Tables 14 and 15. Only slurries with 70 and 75 weight percent powder were investigated using reprocessed powder. The data are plotted in Figures 15 and 16 and appear quite regular, more so than the data on as-received powder of Figure 8. The shrinkages were calculated and are listed in Table 16. The relationship between blade height and shrinkage which was obscure in Table 6 becomes apparent here. As the blade height is increased, the drying shrinkage decreases indicating more tape porosity at larger blade heights. This effect is balanced by increased lamination shrinkage for alrger blade heights. The fact tht the fired density is relatively insensitive to doctor blade height indicates that the particle packing factor is fairly independent of blade height. The transverse shrinkage is fairly consistent for the 70 wt% PZT slurries. More variability is apparent in the 75 wt% slurry, but this could be because each value represents data from only one tape.

Table 14. Thickness and density of tape and green and fired laminates from 70 wt% solids slurries prepared from reprocessed powder.

| Slurry No. | Weight % Solids | Blade Height (mils) | Layer Thickness ± S.D. (mils) Dry Tape | Green Laminate | Fired Multilayer | Density ± S.D. ($gm/cm^2$) Tape (Geom.) | Lam. (Geom.) | Fired (Imer.) | Fired % Theo. | Comment |
|---|---|---|---|---|---|---|---|---|---|---|
| H-20 | 69.9 | 30 | 13.1±0.5 | -- -- | -- -- | -- -- | -- | -- | -- | |
| H-21a | 69.9 | 30 | 14.3±0.4 | -- -- | -- -- | 4.01±0.03 | -- | -- | -- | To H.C.C. |
| H-21b | 69.9 | 30 | 12.3±0.8 | -- -- | -- -- | 4.01±0.03 | -- | -- | -- | (21') |
| H-23 | 70.0 | 30 | 11.7±0.3 | 10.1 -- | 8.5 -- | 4.25±0.03 | 4.92 | 7.63 | 95.8 | Thickness Calibration |
| H-24 | 70.0 | 20 | 7.9±0.3 | 6.8 -- | 5.8 -- | 4.19±0.05 | 4.82 | 7.58 | 95.6 | Thickness Calibration |
| H-24 | 70.0 | 40 | 18.7±0.5 | 15.4 -- | 13.0 -- | 4.35±0.06 | 4.85 | 7.69 | 96.0 | Thickness Calibration |
| H-25 | 70.0 | -- | -- -- | -- -- | -- -- | -- -- | -- | -- | -- | Viscosity Test |
| H-26 | 70.0 | 30 | -- -- | -- -- | -- -- | -- -- | -- | -- | -- | To H.C.C. |
| H-27 | 70.0 | 30 | 12.7±0.5 | -- -- | -- -- | 4.27±0.04 | -- | -- | -- | (26') |
| H-28 | 70.0 | 10 | 3.0±0.2 | 2.7±0.4 | 2.2±1.0 | 3.87±0.09 | 4.56 | 7.65 | 95.6 | Casting rate |
| H-30 | 70.0 | 20 | 7.6±0.3 | 6.5±0.8 | 5.4±0.3 | 4.14±0.04 | 4.80 | 7.50 | 93.8 | Thickness Calibration |
| H-31 | 70.0 | 10 | 3.4±0.1 | 2.9±1.6 | 2.5±0.8 | 4.20±0.06 | 4.74 | 7.61 | 95.1 | Casting rate |
| H-32 | 70.0 | 30 | 12.7±0.2 | 11.1±0.4 | 9.5±0.2 | 4.42±0.06 | 4.88 | 7.60 | 95.0 | To H.C.C. |
| H-33 | 70.0 | 30 | 12.7±0.2 | 11.1±0.4 | 9.5±0.2 | 4.42±0.06 | 4.88 | 7.60 | 95.0 | (25') |
| H-34 | 70.0 | 30 | -- -- | -- -- | -- -- | -- -- | -- | -- | -- | To H.C.C. |
| H-35 | 69.9 | 30 | 11.1±0.2 | 9.61±0.4 | 8.11±0.4 | 4.24±0.13 | 4.81 | 7.62 | 95.3 | (40') |
| H-36 | 70.0 | 30 | 11.5±0.3 | 9.92±0.4 | 8.39±0.8 | 4.25±0.02 | 4.83 | 7.64 | 95.5 | |
| H-37 | 70.0 | 30 | 12.1±0.9 | 10.55±1.2 | 9.02±0.8 | 4.31±0.08 | 4.93 | 7.63 | 95.4 | |
| | | | | | Mean Values | | | | | |
| | 70.0 | 10 | 3.2±0.4 | 2.8±0.1 | 2.4±0.2 | 4.04±0.23 | 4.65 | 7.63 | 95.4 | |
| | 70.0 | 20 | 7.8±0.2 | 6.7±0.2 | 5.6±0.3 | 4.17±0.04 | 4.81 | 7.54 | 94.3 | |
| | 70.0 | 30 | 12.4±1.0 | 10.3±0.6 | 8.7±0.5 | 4.25±0.12 | 4.87 | 7.62 | 95.3 | |
| | 70.0 | 40 | 18.7±0.5 | 15.4 -- | 13.0 -- | 4.35 -- | 4.85 | 7.69 | 96.0 | |

Note: Slip filtered 200 mesh, casting rate 40 in/min., laminated under vacuum.

Table 15. Thickness and density of tape and green and fired laminates from 75 wt% solids slurries prepared from reprocessed powder.

| Slurry No. | Weight % Solids | Blade Height (mils) | Layer Thickness ± S.D. (mils) | | | Density ± S.D. ($gm/cm^2$) | | | Fired % Theo. | Comment |
|---|---|---|---|---|---|---|---|---|---|---|
| | | | Dry Tape | Green Laminate | Fired Multilayer | Tape (Geom.) | Lam (Geom.) | Fired (Immer.) | | |
| H-22 | 75.0 | 20 | 7.3±0.1 | 6.5 | 5.5 | 4.23±0.07 | 4.70 | 7.64 | 95.5 | |
| | | 25 | 11.0±0.4 | 9.8 | 8.3 | 4.23±0.08 | 4.70 | 7.65 | 95.6 | |
| | | 30 | 12.8±0.3 | 11.4 | 9.6 | 4.25±0.04 | 4.81 | 7.65 | 95.6 | |
| | | 40 | 19.2±0.4 | 17.2 | 14.6 | 4.34±0.02 | 4.74 | 7.64 | 95.5 | |
| | | 50 | 26.4±1.2 | 21.7 | 18.5 | 4.39±0.01 | 4.80 | 7.62 | 95.2 | |
| H-29 | 75.0 | -- | -- -- | -- | -- | -- -- | -- | -- | -- | Visc. Test |

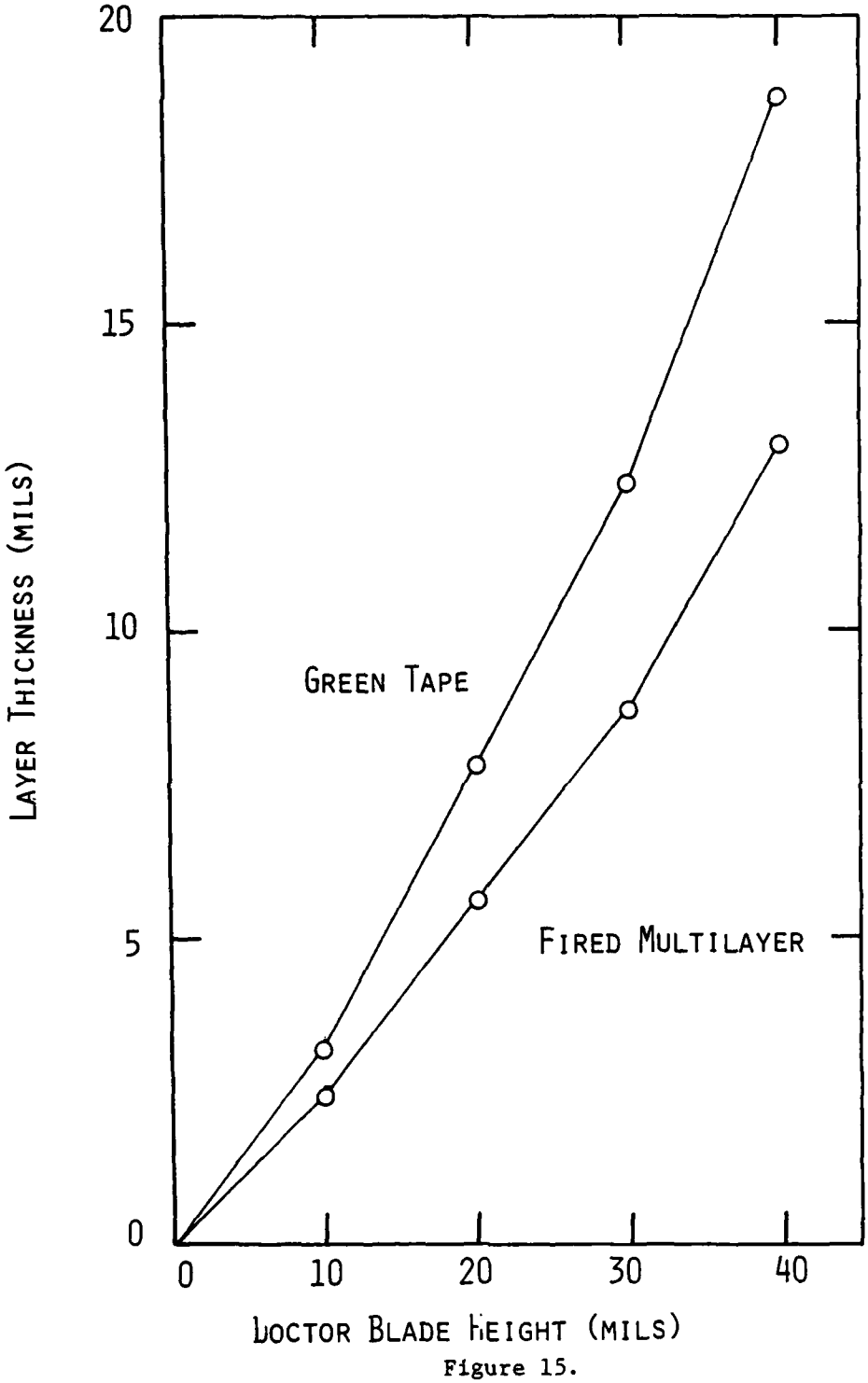
20
15
10
5
0
LAYER THICKNESS (MILS)
GREEN TAPE
FIRED MULTILAYER
0
10
20
30
40
DOCTOR BLADE HEIGHT (MILS)

Figure 15.

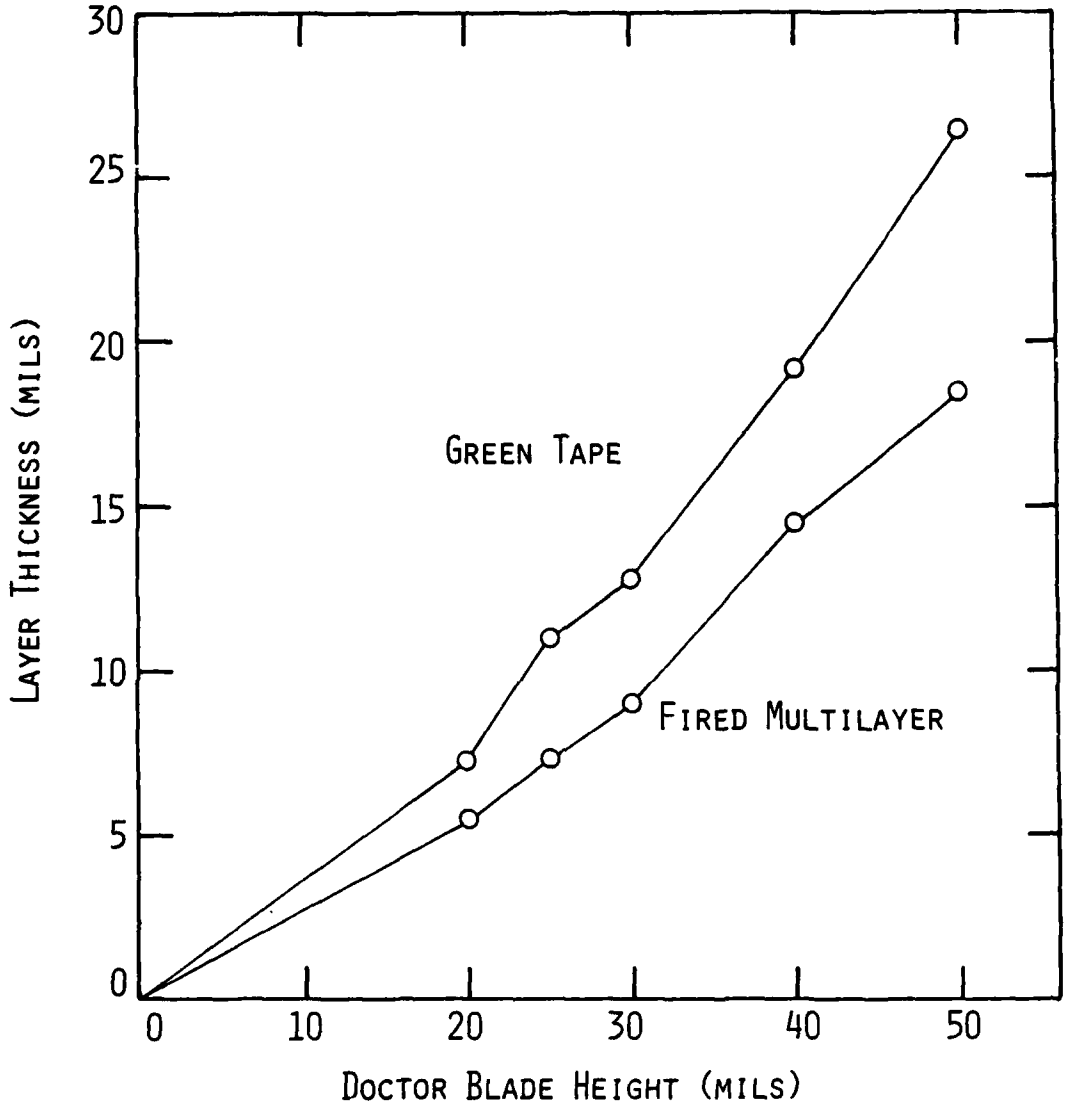
30
25
20
15
10
5
0
0
10
20
30
40
50
LAYER THICKNESS (MILS)
DOCTOR BLADE HEIGHT (MILS)
GREEN TAPE
FIRED MULTILAYER

Figure 16.

Table 16. Shrinkage of reprocessed powder samples.

| Solids Loading (wt%) | Blade Height (mils) | Percent Thickness Shrinkage | | | | Fired Percent Theo. Density | Transverse Shrinkage Re:Lam. % |
|---|---|---|---|---|---|---|---|
| | | Tape Resp. Blade | Lam. Resp. Tape | Fired Resp. Tape | Fired Resp. Blade | | |
| 70.0 | 10 | 68.0 | 12.5 | 14.3 | 76.0 | 95.4 | 15.19 |
| | 20 | 61.0 | 14.1 | 16.4 | 72.0 | 94.3 | 14.66 |
| | 30 | 58.7 | 16.9 | 15.5 | 71.0 | 95.3 | 14.87 |
| | 40 | 53.3 | 17.7 | 15.6 | 67.5 | 96.0 | 14.69 |
| (mean) | | (60.3) | (15.3) | (15.5) | (71.6) | (95.3) | (14.85) |
| 75.0 | 20 | 63.5 | 11.0 | 24.7 | 72.5 | 95.5 | 15.29 |
| | 25 | 56.0 | 10.9 | 24.6 | 66.8 | 95.6 | 15.01 |
| | 30 | 57.3 | 10.9 | 25.0 | 68.0 | 95.6 | 12.89 |
| | 40 | 52.0 | 10.4 | 24.0 | 63.5 | 95.5 | 17.52 |
| | 50 | 47.2 | 17.8 | 29.9 | 63.0 | 95.2 | 12.43 |
| (mean) | | (55.2) | (12.2) | (25.6) | (66.8) | (95.5) | (14.62) |

## 5.3 Effects of Casting Rate on Tape Properties

A test was conducted to determine whether the shear rate in casting would affect the properties of the tape. Carrier speeds from 16 in/min to 60 in/min were investigated for a 10 mil blade height for a 90 wt% solids slurry (H-31). The shear rate at the doctor blade varied from 26.7 to 100 reciprocal seconds. Figure 17 shows the effect of shear rate during casting on the layer thickness and density of tape and multilayers.

A variation of 75 reciprocal seconds in shear (about 45 rpm) results in a variation in fired thickness of about 0.3 mils (about 11 percent of the final thickness). Shear rate has little effect on the fired density of the material. It was suspected that the shear rate might have an effect on the packing factor of the particles. This may still be true in the case of non-equiaxed particulates. The insensitivity of the density to shear leads us to believe that the variation in thickness is due to surface tension effects between the slurry and the doctor blade. The effect should be quite reproducible if slurry viscosity is under control.

## 6.0 Binder Burnout Testing

As requested by Honeywell Ceramics Center, thermoanalytical testing was performed on the pure dried Cladan binder CB73115. Figure 18 shows a differential thermal analysis in static air at a heating rate of 3°C/min. Exothermic peaks occur at 185, 310, 390 and 440°C. Figure 19 shows thermogravimetric analysis at heating rates of 3 and 5°C/min in static air and 10°C/min in flowing air. The results are difficult to interpret. We would expect weight loss to occur at lower temperatures for slower heating rates. We would also expect air flow to accelerate weight loss and move the curve to lower temperatures. The reversal of the 3 and 5°C/min heating rates is the most troubling.

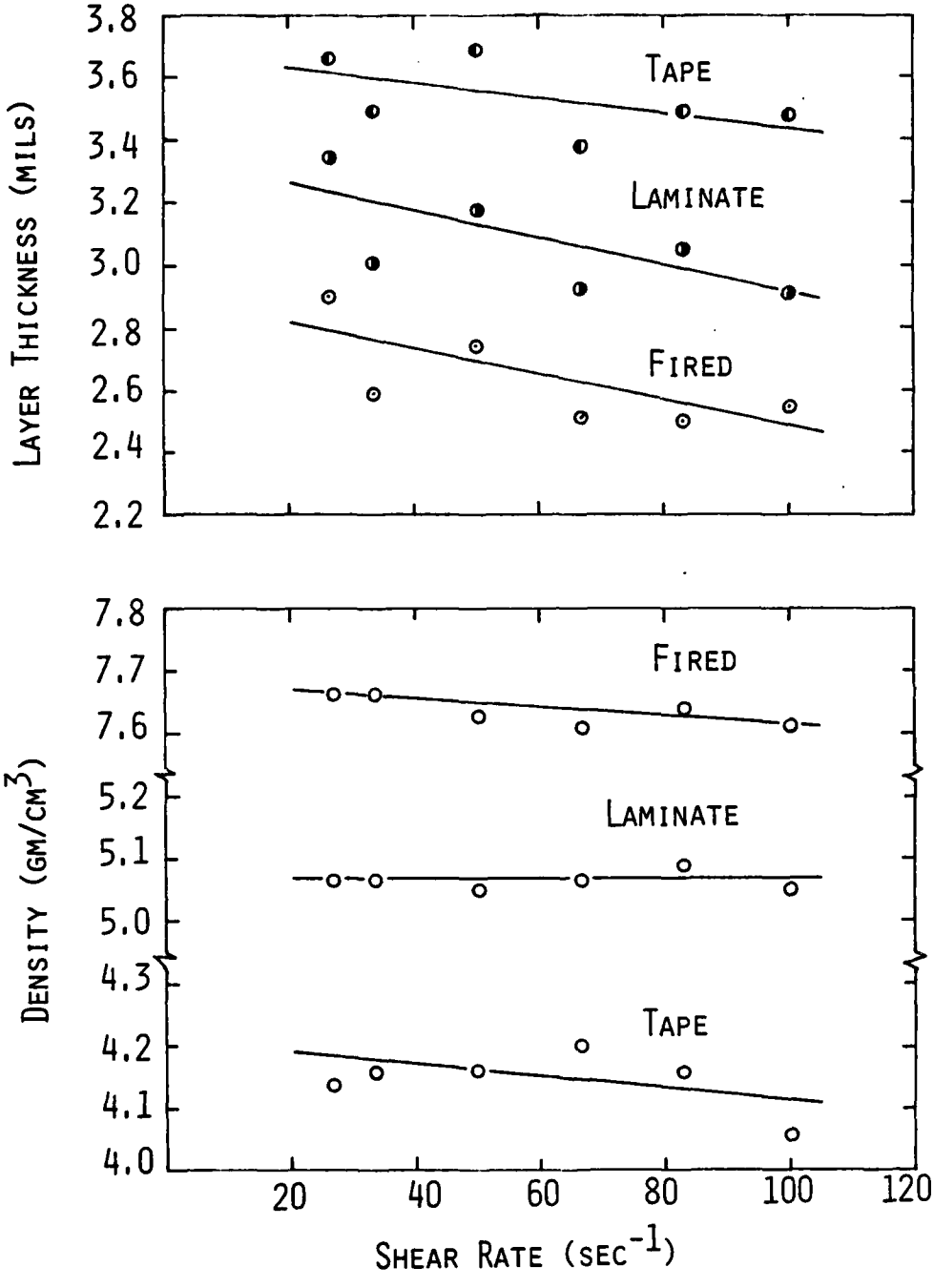
LAYER THICKNESS (MILS)
3.8
3.6
3.4
3.2
3.0
2.8
2.6
2.4
2.2
TAPE
LAMINATE
FIRED
DENSITY (GM/CM3)
7.8
7.7
7.6
5.2
5.1
5.0
4.3
4.2
4.1
4.0
FIRED
LAMINATE
TAPE
20
40
60
80
100
120
SHEAR RATE (SEC-1)

Figure 17.

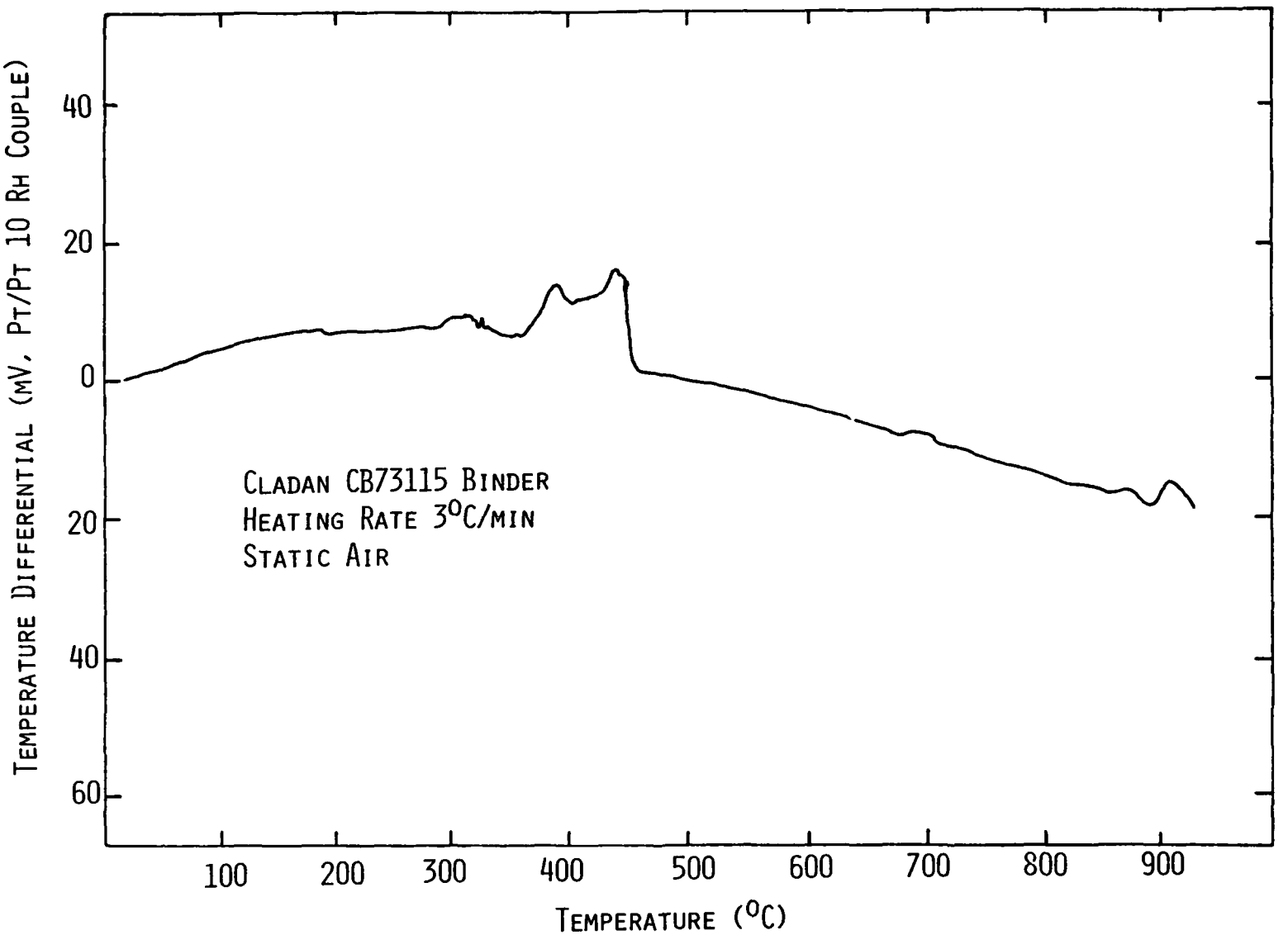
Temperature Differential (mV, Pt/Pt 10 Rh Couple)
40
20
0
20
40
60
Cladan CB73115 Binder
Heating Rate 3°C/min
Static Air
100
200
300
400
500
600
700
800
900
Temperature (°C)

Figure 18.

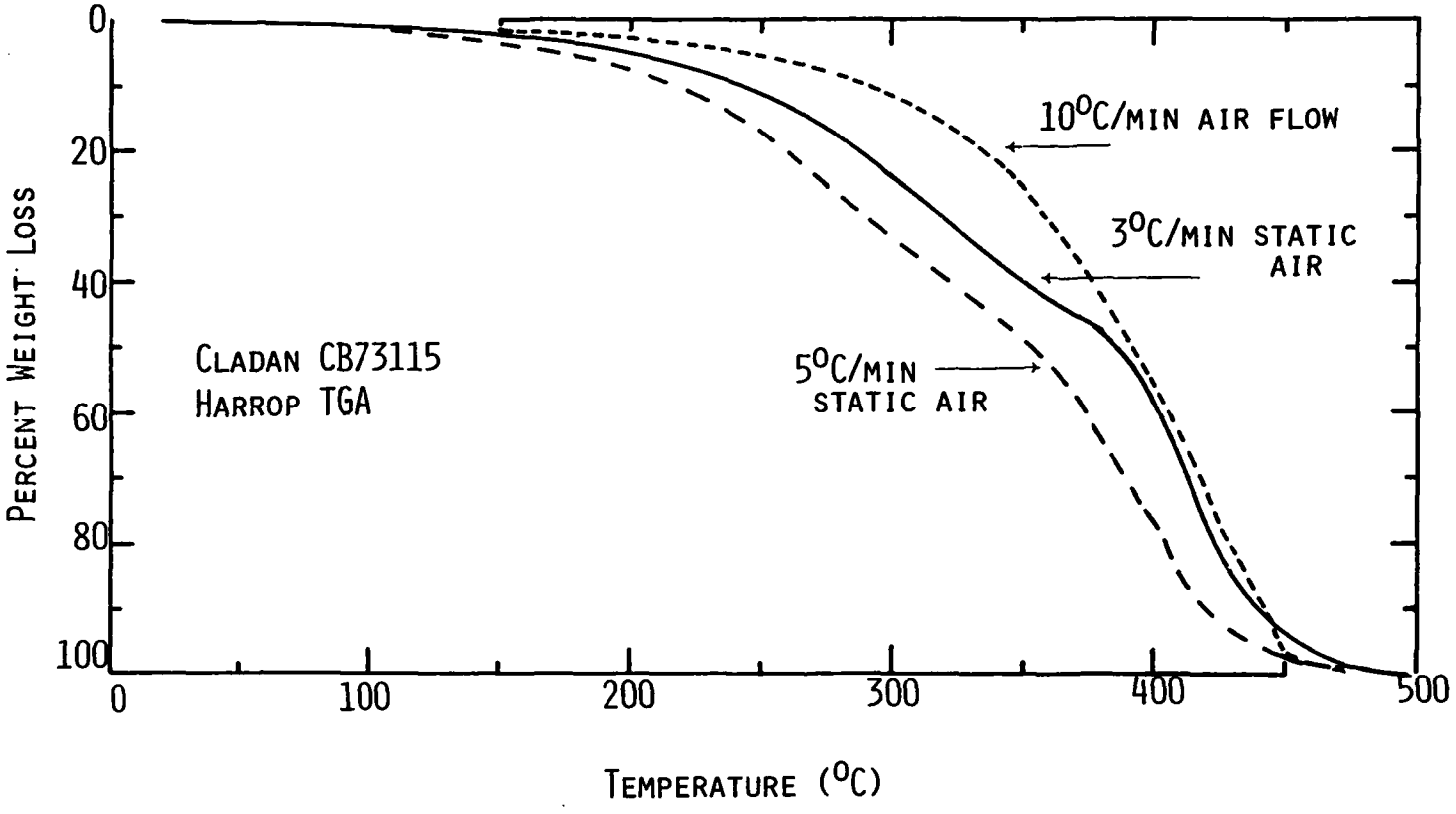
0
20
40
60
80
100
PERCENT WEIGHT LOSS
CLADAN CB73115
HARROP TGA
10°C/MIN AIR FLOW
3°C/MIN STATIC AIR
5°C/MIN STATIC AIR
0
100
200
300
400
500
TEMPERATURE (°C)

Figure 19.

Using the 5°C/min curve 180, 300 and 375°C were picked as critical weight loss temperatures. Another TGA run was done and program holds were initiated at these temperatures while weight loss was monitored on a time base recorder. The results are shown in Figure 20. It would appear that a 15 hour hold at 180°C and a 10 hour hold at 300 with moderately slow heating in between and up to the maximum temperature would account for most of the burnout required by the pure binder.

## 7.0 Conclusions

The results of this work indicate several points that are important to the tape casting process.

1. The agglomeration nature of the powder both in its dry form and in the casting slurry is significant in determining the packing of particles in the green tape and affect the density of the fired multilayer. It is very possible that the best way to optimize the agglomeration nature of the powder is to use a two step milling process, where agglomeration is controlled by milling time in the low-viscosity solvent portion of the system and the high-viscosity binder components are added prior to a second milling step.
2. Measurement and control of slurry viscosity (and slurry density) are important to reproducibility in thickness and density of the final product. (Temperature of the slurry during casting can and often is used to control viscosity in production scale processes.) A slip conditioning station near the casting head has been discussed and should be incorporated into the Honeywell equipment. The slip container shoudk be constantly stirred at low rpm, its viscosity continuously monitored, and its temperature should be variable to control viscosity.

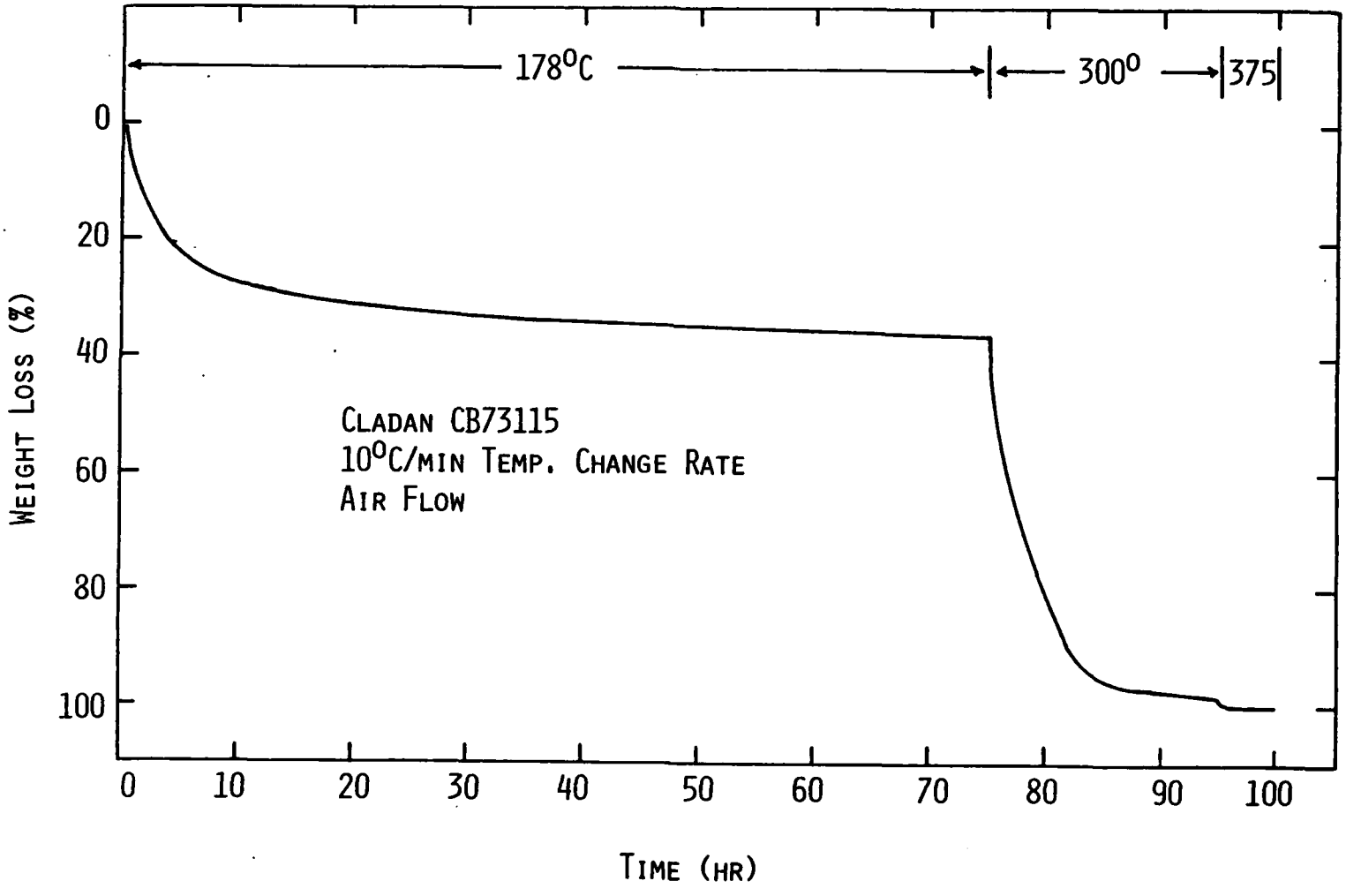
178°C
300°
375
0
20
40
60
80
100
WEIGHT LOSS (%)
CLADAN CB73115
10°C/MIN TEMP. CHANGE RATE
AIR FLOW
0
10
20
30
40
50
60
70
80
90
100
TIME (HR)

Figure 20.

3. Choice of powder loadings should be made to avoid compositions where small changes in solids content cause dramatic changes in viscosity, while still achieving the best possible fired density.
4. Production of tape in small lots as was done for this study is not conducive to achieving the best reproducibility. It should not be forgotten that these results represent only a baseline for starting a production type process. Many second order effects such as slurry temperature, casting speed, drying time, etc. are best optimized under production conditions.

## References


1. Liebedzik, J., Burke, R.G., et al., pp. 121-128 in Proceedings of the 6th Annual Scanning Electron Microscope Symposium, O. Johari and I. Corvin, eds., IIT Research Inst., Chicago, IL (1973).
2. Brunower, S., Emmett, P and Teller, E., J. Am. Ceram. Soc. 60:309 (1938).
3. Sikdar, S.K. and Ore, F., Viscosity Measurements of Non-Newtonian Slurry Suspensions Using Rotating Viscometers, Ind. Eng. Chem. Process Des. Dev., 18(4):722-726 (1979).
4. Brookfield Laboratories (personal communication).

# DEPARTMENT OF THE NAVY

OFFICE OF NAVAL RESEARCH
ARLINGTON, VIRGINIA 22217

IN REPLY REFER TO

## BASIC DISTRIBUTION LIST

Technical and Summary Reports December 1982

| Organization | Codes |
|---|---|
| Defense Documentation Center<br>Cameron Station<br>Alexandria, VA 22314 | 12 |
| Office of Naval Research<br>Department of the Navy<br>800 N. Quincy Street<br>Arlington, VA 22217<br>Attn: Code 431 | 3 |
| Naval Research Laboratory<br>Washington, DC 20375<br>ATTN: Codes 6000<br>6300<br>2627 | 1<br>1<br>1 |
| Naval Air Development Center<br>Code 606<br>Warminster, PA 18974<br>ATTN: Dr. J. DeLuccia | 1 |
| Commanding Officer<br>Naval Surface Weapons Center<br>White Oak Laboratory<br>Silver Spring, MD 20910<br>ATTN: Library | 1 |
| Naval Oceans Systems Center<br>San Diego, CA 92132<br>ATTN: Library | 1 |
| Naval Postgraduate School<br>Monterey, CA 93940<br>ATTN: Mechanical Engineering Department | 1 |
| Naval Air Systems Command<br>Washington, DC 20360<br>ATTN: Code 31A<br>Code 5304B | 1<br>1 |
| Naval Sea System Command<br>Washington, DC 20362<br>ATTN: Code 05R | 1 |

| Organization | Copies |
|---|---|
| Naval Air Propulsion Test Center<br>Trenton, NJ 08628<br>ATTN: Library | 1 |
| Naval Construction Battallion<br>Civil Engineering Laboratory<br>Port Hueneme, CA 93043<br>ATTN: Materials Division | 1 |
| Naval Electronics Laboratory<br>San Diego, CA 92152<br>ATTN: Electron Materials Sciences Division | 1 |
| Naval Missile Center<br>Materials Consultant<br>Code 3312-1<br>Point Mugu, CA 92041 | 1 |
| Commander<br>David W. Taylor Naval Ship Research and Development Center<br>Bethesda, MD 20084 | 1 |
| Naval Underwater System Center<br>Newport, RI 02840<br>ATTN: Library | 1 |
| Naval Weapons Center<br>China Lake, CA 93555<br>ATTN: Library | 1 |
| NASA<br>Lewis Research Center<br>21000 Brookpark Road<br>Cleveland, OH 44135<br>ATTN: Library | 1 |
| National Bureau of Standards<br>Washington, DC 20234<br>ATTN: Metals Science and Standards Division<br>Ceramics Glass and Solid State Science Division<br>Fracture and Deformation Div. | 1<br>1<br>1 |

Naval Facilities Engineering Command
Alexandria, VA 22331
ATTN: Code 03 1

Scientific Advisor
Commandant of the Marine Corps
Washington, DC 20380
ATTN: Code AX 1

Army Research Office
P. O. Box 12211
Triangle Park, NC 27709
ATTN: Metallurgy & Ceramics Program 1

Army Materials and Mechanics Research Center
Watertown, MA 02172
ATTN: Research Programs Office

Air Force Office of Scientific Research/NE
Building 410
Bolling Air Force Base
Washington, DC 20332
ATTN: Electronics & Materials Science Directorate 1

NASA Headquarters
Washington, DC 20546
ATTN: Code RRM 1

Defense Metals and Ceramics Information Center
Battelle Memorial Institute
505 King Avenue
Columbus, OH 43201 1

Metals and Ceramics Division
Oak Ridge National Laboratory
P.O. Box X
Oak Ridge, TN 37380 1

Los Alamos Scientific Laboratory
P.O. Box 1663
Los Alamos, NM 87544
ATTN: Report Librarian 1

Argonne National Laboratory
Metallurgy Division
P.O. Box 229
Lemont, IL 60439 1

Brookhaven National Laboratory
Technical Information Division
Upton, Long Island
New York 11973
ATTN: Research Library 1

Library
Building 50, Room 134
Lawrence Radiation Laboratory
Berkeley, CA 1

Send ONE COPY to each unless otherwise indicated.

# SUPPLEMENTARY DISTRIBUTION LIST A
## Electronic, Magnetic, and Optical Ceramics

Revision of Supp. List A
(Electronic, Magnetic & Optical Ceramics)

Advanced Research Projects Agency
Materials Science Director
1400 Wilson Boulevard
Arlington, VA 22209

Don Berlincourt
Channel Products
7100 Wilson Mills Rd.
Chesterland, OH 44026

Dr. C. M. Stickley, V.P.
The BDM Corporation
7915 Jones Branch Drive
McLean, VA 22102

Dr. Robert Callahan
Channel Industries
339 Ward Drive
Box 3680
Santa Barbara, Ca 93105

Professor L. E. Cross
The Pennsylvania State University
Materials Research Laboratory
University Park, PA 16802

Mr. C. LeBlanc
Naval Underwater Systems Center
New London Laboratory 3224
New London, CT 06320

Dr. Frank Recny
General Electric Co.
Bldg. 5 Room 8
Electronics Park
Syracuse NY 13201

Dr. J. H. Rosolowski
General Electric Company
Research and Development Center
P.O. Box 8
Schenectady, NY 02301

Dr. Gene Haertling
Motorola Corporation
3434 Vassar, NE
Albuquerque, NM 87107

W.B. Harrison
Honeywell Ceramics Center
5121 Winnetka Ave. N.
New Hope MN 55428

Dr. Gordon R. Love
Corporate Research, Development
and Engineering
Sprague Electric Co.
North Adams, Mass 01247

Dr. B.G. Koepke
Honeywell Ceramic Center
5121 Winnetka Ave.N.
New Hope, MN 55428

Dr. R. Lapetina
Edo Western Corporation
2645 South 300 West
Salt Lake City, UT 84115

Professor R. Roy
The Pennsylvania State University
Materials Research Laboratory
University Park, PA 16802

Dr. N. Tallan
AFML Wright-Patterson AFB
Dayton, OH 45433

Dr. H. E. Bennett
Naval Weapons Center
Code 3818
China Lake, CA 93555

Dr. K. D. McHenry
Honeywell Ceramics Center
[illegible] Winnetka ave., N.
New Hope, MN 55428

Dr. Lew Hoffman
Hoffman Associates
301 Broadway (US 1) Suite 206A
P.O. 10492
Riviera Beach, FL 33404

Roger T. Dirstine
Ceramics Research
Unitrode Corporation
580 Pleasant St.
Watertown, Mass 02172

Dr. Paul D. Wilcox
Sandia Laboratories
Division 2521
Albuquerque, NM 87115

Dr. R. Rice
Naval Research Laboratory
Code 6360
Washington, DC 20375

Dr. George W. Taylor
Princeton Resources, Inc.
P.O. Box 211
Princeton NJ 08540

Dr. Herb Moss
RCA Laboratories
Princetown, NJ 08540

Dr. C. Hicks
Code 631
Naval Ocean Systems Center
San Diego, CA 92152

John Piper
Union Carbide Corporation
Electronics Division-Components Dept.
P.O. Box 5928
Greenville, SC 29606

[illegible] Whang
Technical Center
[illegible] Corporation
[illegible] E. Pleasant Valley Road
Independence, OH 44131

Dr. R. Bratton
Westinghouse Research Laboratory
Pittsburgh, PA 15235

Dr. James Pappis
Raytheon Co., Research Division
28 Seyon Street
Waltham, MA 02154

Dr. Perry A. Miles
Raytheon Co., Research Division
28 Seyon Street
Waltham, MA 02154

Dr. P. E. D. Morgan
Rockwell Science Center
1049 Camino Dos Rios
P.O. Box 1085
Thousand Oaks, CA 91360

Dr. G. Ewell
MS6-D163
Hughes Aircraft Company
Centinela & Teale Streets
Culver City, CA 90230

Dr. S.K. Kurtz, V.P.
Clairol, Inc.
2 Blachley Road
Stamford, CT 06902

Dr. D. Carson
Code 7122
Naval Ocean Systems Center
San Diego, Ca 92152

Dr. J. Smith
GTE Sylvania
100 Endicott Street
Danvers, MA 01923

Dr. Wallace A. Smith
North American Philips Laboratories
345 Scarborough Road
Briarcliff Manor, NY 10510

Dr. S. Musikant
General Electric Co.
3188 Chestnut Street
Philadelphia, PA 19101

Dr. Manfred Kahn
Code 6360
US Naval Research Laboratory
Washington, DC 20375

Mr. G. Goodman, Manager
Corporation of Applied Research
Group
Globe-Union Inc.
5757 North Green Bay Avenue
Milwaukee, WI 53201

Dr. J. V. Biggers
Pennsylvania State University
Materials Research Laboratory
University Park, PA 16802

Army Research Office
Box CM, Duke Station
Attn: Met. & Ceram. Div.
Durham, NC 27706

Dr. R. N. Katz
Army Materials and Mechanics
Research Center
Watertown, MA 02171

Dr. Kim Ritchie
Vice President
Corporate Research Laboratory
AVX Corporation
P.O. Box 867
Myrtle Beach, SC 29577

Advanced Research Projects
Materials Science Director
1400 Wilson Boulevard
Arlington, VA 22209

Dr. A. Gentile
Hughes Research Laboratories
3011 Malibu Canyon Road
Malibu, CA 90265

John C. Constantine
Electronic Materials Systems
Englehard Industries Division
1 West Central Ave.
E. Newark, NJ 07029

Director
Applied Research Lab
The Pennsylvania State University
University Park, PA 16802

Dr. Sidney J. Stein
Electro-Science Laboratories
2211 Sherman Ave
Pennsauken, NJ 08110

Dr. F. F. Lange
Rockwell International
P.O. Box 1085
1049 Camino Dos Rio
Thousand Oaks, CA 91360

Dr. R.R. Neurgaonkar
Rockwell International Sciences Center
1049 Camino Dos Rios
P.O. Box 1085
Thousand Oaks, CA 91360

W.B. Harrison
Honeywell Ceramics Center
5121 Winnetka Ave. N.
New Hope, MN 55428

Dr. P.L. Smith
Naval Research Laboratory
Code 6361
Washington, DC 20375

END

FILMED

8-83

DTIC